NUMERICAL SIMULATIONS ON A CENTRIFUGAL PUMP OPERATING IN TURBINE MODE

José David Villegas Jiménez

EAFIT UNIVERSITY

ENGINEERING SCHOOL

MECHANICAL ENGINEERING DEPARTMENT

MEDELLIN

2010

NUMERICAL SIMULATIONS ON A CENTRIFUGAL PUMP OPERATING IN TURBINE MODE

Graduation project for the degree of Mechanical Engineer

Advisor

MSc. Santiago Orrego Bustamante

EAFIT UNIVERSITY

ENGINEERING SCHOOL

MECHANICAL ENGINEERING DEPARTMENT

MEDELLIN

2010

To my family for giving me all the support I needed during all these years.

Acknowledgments

“I would like to thank my family for all the effort, patience and support during this educational process. It is important to thank the Hydraulic and Metrology laboratories of EAFIT University for the necessary equipment and support to complete the project, as well as classmate and friend Sebastian Sierra P., for helping me with reverse engineering process. I would like to express my gratitude to my advisor, Santiago Orrego for the support and patience in the accomplishment of diverse tasks in the project and all the guys from the Applied Mechanics Laboratory for being always kind and making the workplace a funny place to be.”

Abstract

The project presents the study of a centrifugal pump operating in turbine mode as an alternative in micro power generation for isolated regions of Antioquia that are not connected to the national energy network. The use of engineering knowledge as well as powerful computational resources permit development of solutions for environmental problems like the present case where a great amount of people might benefit from natural resources. In the project, computational models were obtained by reverse engineering techniques in order to perform CFD simulations at several conditions for a centrifugal pump when operated in reverse behavior (Flow rate and total head at angular velocity of $1750[rpm]$) . The objective was to find best operation values, able to generate electricity [$1.5kW$], by means of maximum efficiency in reverse operation of the pump. The results were plotted and compared with experimental methods proposed by researchers worldwide.

Keywords: *Centrifugal pump, flow rate, Best Efficiency point, CFD*

CONTENTS

LIST OF TABLES

LIST OF FIGURES

LIST OF SYMBOLS

Q	Flow rate
H	Total Head
P	Pressure
N	Rotational speed
N_s	Specific speed
γ	Specific weight
η	Efficiency
ρ	Density
τ	Torque
ω	Angular velocity
V	Velocity
g	Gravity
z	Elevation head
k	Turbulence Kinetic energy
ε	Turbulent dissipation energy
U	Tangential velocity
D	Impeller diameter
P_p	Pump input power
P_h	Hydraulic power
P_m	Mechanic power
P_{elec}	Electrical power
Π	Power dimensionless coefficient
Φ	Flow dimensionless coefficient
Ψ	Head dimensionless coefficient

1 INTRODUCTION

The large variety of knowledge applied in Engineering permit to find out solutions to daily problems, based on requirements and analyzed from a critical point of view. Nowadays,different methods are used to solve problems in less time by means of numerical simulations of physical phenomena inside a virtual and interactive environment.

During last years the struggle for good energy disposal and administration has created a great interest among different people to make it renewable, facing an increasing environmental crisis. It is well known that electrical energy permits people to have better life conditions. Unfortunately, in Antioquia there are still isolated places without the possibility to acquire this resource. Rural zones not connected to the national energy network reveal an opportunity where solutions are meant to be found. Studies in technology mixed with correct physical principles formulations can reveal better analysis for the problem in question.

According to the described issue, the study of electrical energy generation by operating a centrifugal pump in turbine mode is intended. This can be done reversing the pump principle for turbine operation and analyzing its behavior with computational tools.

A hydraulic pump is basically, a device that receives mechanical energy from an external source and transforms it into hydraulic energy in order to provide movement to a fluid.

Hydraulic pumps origin is claimed to Greek mathematician, Archimedes of Syracuse and his invention; a rotating screw inside a closed cylinder on a sloping plane able to

transport a fluid from one point to another.The concept of this first pump has evolved and extended for several industrial processes.

Since this discovery, several types of hydraulic pumps had been developed using analytical solutions of physical phenomena, experimentation and recently, trendy computational alternatives.

Computational tools for fluid movement analysis are being used as support for fluid-solid interaction in external domains like an airplane wing profile, or internal domains like the flow inside a pipe. The CFD (Computational Fluid Dynamics) methods are the basis for a meticulous analysis of elements that involve solid, fluid and gas interaction.

The use of CFD methods for the mentioned problem is the key to develop a great study of the device, fitting a physical-mathematical model through a simulation in order to achieve interesting results.

2 JUSTIFICATION

The need of energy has taken human beings one step forward inside the search of new energy sources and the best way to take advantage of them. Traditional ways for energy transformation such as chemical–mechanical interaction in combustion engines, electrical–thermal interaction in ovens, electrical–mechanical interaction in home electrical appliances, etc. are reducing their participation in global development context, due to the environmental trouble they generate.

In the discussion about energy situation in developed countries, particularly inside rural areas, the small hydraulic electric power stations play an important role for the development of the region. The high budget of initial investment is a disadvantage for the construction of these power stations. This situation can be faced up by using centrifugal pumps operating in turbine mode. The use of pumps reduces the investment thoroughly.(AUDISIO, 2009)

The idea emerges with the purpose of taking advantage of Antioquia's hydrological resources, specifically the natural movement of rivers and basins by operating a centrifugal pump in turbine mode. This hydrological resource needs to be exploited for the promotion of new technological development inside the affected region as well as for people and small companies benefit. The hydraulics laboratory in EAFIT University is dealing with a research about the behavior of a centrifugal pump operating in turbine mode with aims of obtaining valuable data and documentation for further studies and applications to transform energy efficiently.

The market for centrifugal pumps assures its availability and by the way becoming a guarantee for the investor and the people who will receive the benefits of the project.

3 OBJECTIVES

3.1 **General Objective**

To execute one (1) CFD simulation in steady state, of a centrifugal pump operating in turbine mode and certain working conditions (flow rate, pressure head and revolutions). The pump is installed in the Hydraulics Laboratory of EAFIT University.

3.2 **Specific Objectives**

3.2.1 **Objective 1** To define the state of art in numerical simulations for pumps. Level 1–To know

3.2.2 **Objective 2** To obtain CAD models of pump's necessary components for setting up the simulation. Level 2– To comprehend

3.2.3 **Objective 3** To execute the meshing of pump components. Level 3– To apply.

3.2.4 **Objective 4** To configure simulation parameters and calibration of the CFD model. Level 4– To analyze

3.2.5 **Objective 5** To generate and analyze results. Level 4– To analyze

4 STATE OF ART

In the following pages, a brief description of the main features relating to the project will be fulfilled. General aspects of centrifugal pumps, numerical simulations, and physical theory are going to be explained in order to execute further work during the project development.

4.1 **Centrifugal Pump**

4.1.1 **Definition.** A centrifugal pump is a rotating machine in which flow and pressure are generated dynamically, delivering useful energy to the fluid largely through velocity changes.(KARASSIK et al., 2008) The main purpose of a centrifugal pump is to conduct the fluid from one location to another providing certain amount of energy that is able to overcome resistance from pipes and circulation. A centrifugal pump has two main parts, a rotating component called impeller and a stationary part called volute

Figure 1: Centrifugal Pump

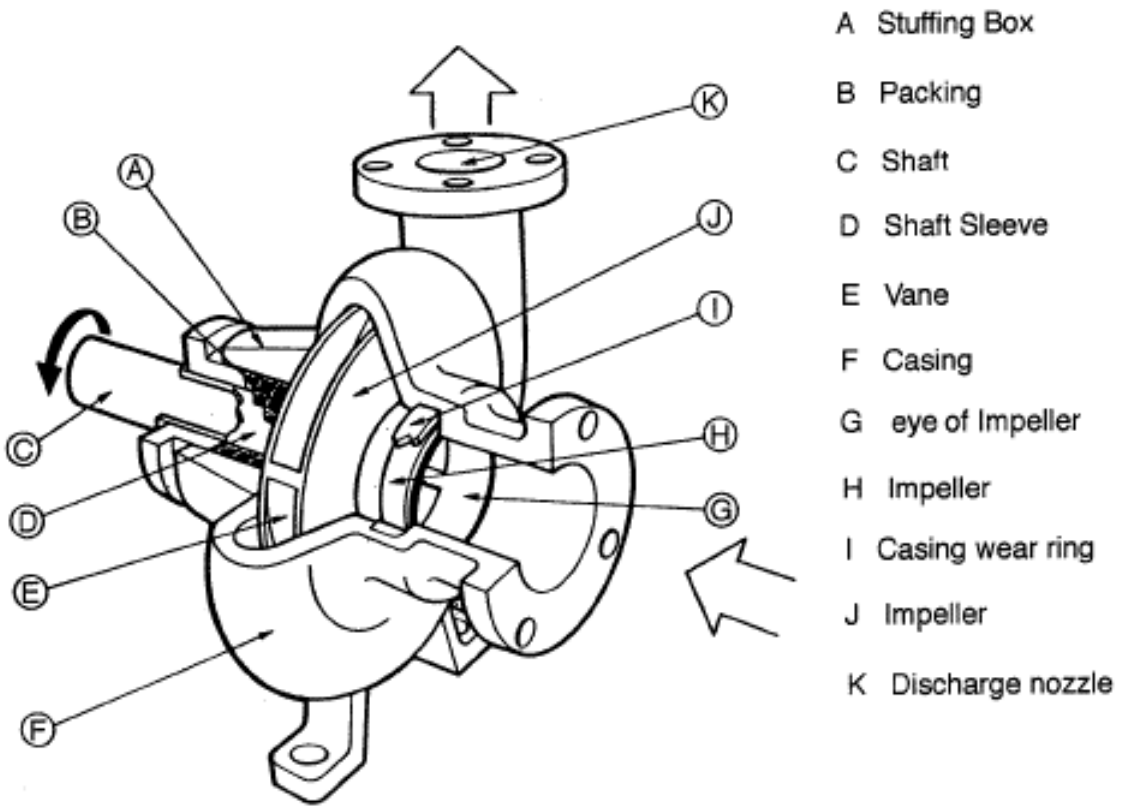

(PUMPWORLD, 2009)

The amount of energy given to the fluid is proportional to the velocity at the edge or vane tip of the impeller. The faster the impeller revolves or the bigger the impeller is, then the higher will be the velocity of the fluid at the vane tip and the greater the energy imparted to the fluid.(SAHDEV, 2009) Main parts of a centrifugal pump can be seen in figure 1 and they will be described in section 4.1.2

The centrifugal force acts while the impeller is rotating. The fluid sitting in the cavities

between the vanes moves outward, imparting centrifugal acceleration and increasing speed at discharge. When the fluid leaves the suction eye of the impeller a low pressure area (vacuum) is created at this location, allowing more fluid to enter the pump inlet.(PUMPWORLD, 2009) The principle of the centrifugal pump can be seen in figure 2

Figure 2: Pump operation schema

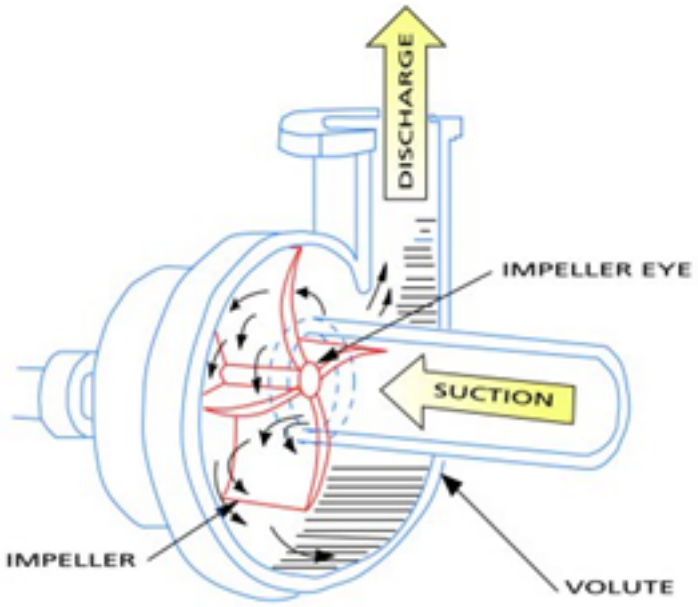

(PUMPWORLD, 2009)

Centrifugal pumps offer several advantages like relative small size, handling of high temperature fluids, no other resistance components required (i.e. valves), no mechanisms neither joints, and the most important, low costs of investment and minimal maintenance costs.

4.1.2 **Centrifugal Pump Parts**

Impeller. The impeller is the rotating part that moves the fluid inside the pump body, providing it with centrifugal acceleration. The shape of the impeller is designed with vanes for guiding the fluid through the volute. They are classified according the purpose and the configuration of the pump:

1. Based on flow direction
    - Radial flow: The fluid enters at the center of the impeller and is directed out along the impeller blades perpendicular to the shaft axis.This configuration provides less flow rate but high values for power
    - Axial flow: The fluid enters at the center of the impeller and is directed out along the impeller blades parallel to the shaft axis. This configuration is intended to provide high flow rate values and less power than a radial configuration
    - Mixed flow: The fluid has a mixed condition of radial and axial flow.
2. Based on suction type
    - Single suction: The flow inlet is situated in one side of the pump
    - Double suction: The flow inlet is situated symmetrically on both sides of the pump
3. Based on mechanical configuration
    - Open: The vanes are exposed. Used for dirty fluids (suspended matter or small particles

- Semi-open: The vanes are not enclosed at all; only one side has a plate. Used for solid fluids with stringy materials.
- Closed: The vanes are enclosed with a plate on both sides. Used for clean fluids. See Figure 3

Figure 3: Impeller Types. Open. Semi-open. Closed

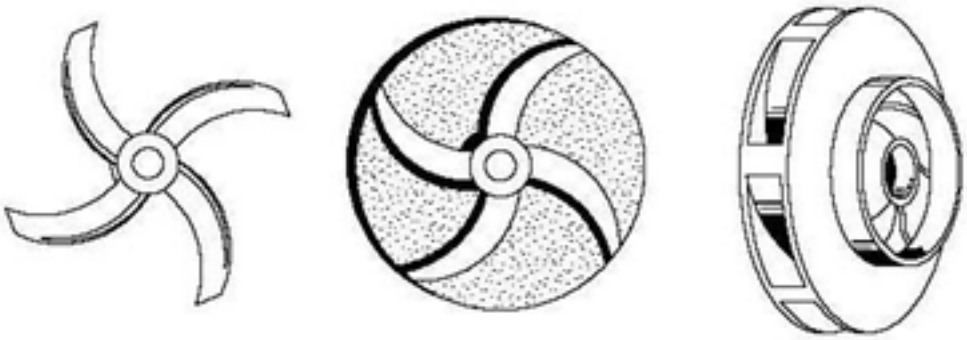

(TPUB,2010)

The project is intended for operating with a closed impeller which is the most universally used.

Volute Casing. A volute is a curved funnel that increases its cross section area as the discharge port is reached. Discharge port is the section of the volute where the flow exits the pump. When the area is bigger the speed of the fluid is reduced and therefore its pressure is increased. The purpose of the volute casing is to balance the hydraulic pressure on the shaft at the designed configuration recommended by the manufacturer. The volute to be used can be seen in figure 4

Figure 4: Volute casing

4.1.3 **Turbomachinery concepts, pump and turbine.** The following concepts are taken and collected from several research documentation and bibliography. They give an idea of main turbomachines theory for better understanding of further computational applications.

Head. The term head is used to measure the kinetic energy which a pump creates. Head is a measurement of the height of the liquid column the pump creates from the kinetic energy the pump gives to the liquid. The main reason for using head instead of pressure to measure centrifugal pump energy is that the head will not change if the specific weight of the fluid (γ) changes, while pressure will.(GOULDS, 2009)

Bernoulli's equation provides a relationship between pressure,velocity and elevation head.

$$\underbrace{H}_{\text{Total developed head}} = \underbrace{\frac{p}{\gamma}}_{\text{Pressure head}} + \underbrace{\frac{V^2}{2g}}_{\text{Velocity head}} + \underbrace{z}_{\text{Elevation head}} \quad (1)$$

This expression provides a relationship between pressure, velocity magnitude and

height above a specified datum plane from which all elevations are measured. For horizontal pumps, this reference line shall be the centerline of the pump shaft. This equation is known as the Bernoulli equation while H is known as the Bernoulli constant or Total Head. First term is the pressure head, second is velocity head and third is elevation head.(STREET et al., 1996)

Head can also be expressed in terms of velocity components inside impeller vanes and in relation to Euler-one dimensional equation

When flow is going through vanes energy transfer is performed. Two consecutive vanes form a duct where fluid circulates take or yield energy by means of machine configuration. If the pump operates in normal mode, energy is given to the vanes while in reverse action the fluid transfer energy to the impeller and finally to the shaft.The study of the flow through the duct results in vectorial diagrams of velocity inside machine blade system (Runner or Impeller) and into Euler equation. Assuming a control volume for both machines included between inlet (denoted as 1) and outlet (denoted as 2) .Euler equation for both types of machines is:

$$H = \frac{1}{g}\left(U_2 V_{t2} - U_1 V_{t1}\right) \tag{2}$$

where:

H=Head [m]or [ft]

U=Tangential velocity [$\frac{m}{s}$ or $\frac{ft}{s}$]

V=Resulting velocity [$\frac{m}{s}$ or $\frac{ft}{s}$]

1=inlet

2=outlet

This equation has it origin in tangencial velocity changes between fluid and vanes at

impeller or runner outlet and inlet.

Figure 5: Velocity triangles

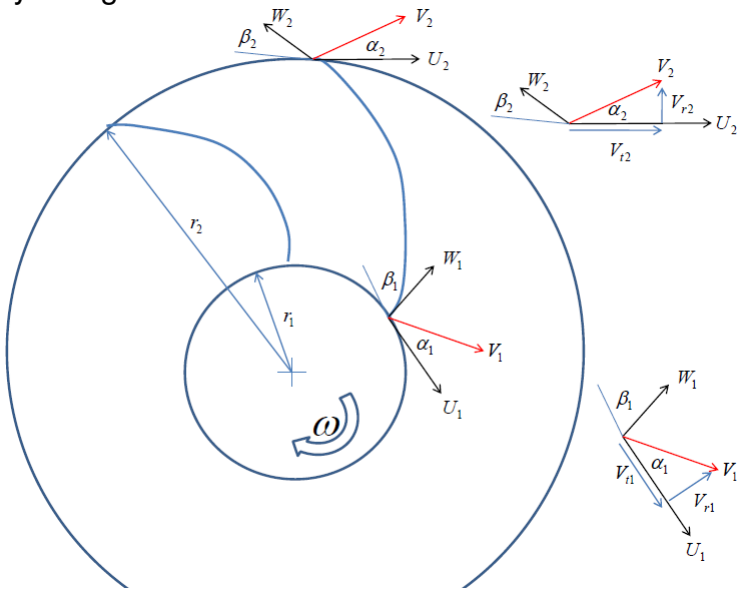

(MUNSON et al., 2002)

Now considering a pump the outlet energy will be greater $(U_2V_{t2} > U_1V_{t1})$ showing a positive value, meaning the work is being made by the shaft. For turbines $(U_1V_{t1} > U_2V_{t2})$ so the work is given to the shaft. (POLO, 1980)

The Euler Head equation for pumps and turbines are respectively:

$$H_p = \frac{1}{g}\left(U_2V_{t2} - U_1V_{t1}\right) \tag{3}$$

$$H_t = \frac{1}{g}\left(U_1V_{t1} - U_2V_{t2}\right) \tag{4}$$

Head increment depends on Q in a linear way for given blade geometry and velocity.

For pumps, the blade angle β_2 varies from $15° - 35°[grad]$ with normal interval of $20° < \beta_2 < 25°$ and $15° < \beta_2 < 50°$. This angle is established at the tip of the vane between the tangential and normal components of the velocity as seen in figure 5

Capacity/Flowrate/Discharge (Q). Capacity means the flow rate with which liquid is moved or pushed by the pump to the desired point in the process. It is commonly measured in either gallons per minute (gpm) or cubic meters per second m^3/s. The capacity of a pump usually changes with different operation conditions of the process depending on factors like:

- Process liquid characteristics i.e. density, viscosity
- Impeller size
- Impeller rotational velocity

Power and efficiency. The work performed by a pump is a function of the total head and the weight of the liquid pumped in a given time period. The pump capacity in gpm and the liquid specific gravity are normally used in the formulas rather than the actual weight of the liquid pumped(GOULDS, 2009)
Pump input power (P_p) or brake horsepower (bhp) is the power delivered to the pump shaft.

$$P_p = bhp = \frac{\gamma Q H}{\eta} \tag{5}$$

where:
Q=Flowrate $[\frac{m^3}{s}] or [gpm]$
H=Head $[m] or [ft]$

γ=Specific weight $\frac{N}{m^3} or \frac{lb}{ft^3}$

η= Pump efficiency

Hydraulic pump power (P_h) or water horsepower (whp) is the power imparted to the liquid by the pump.

$$P_h = whp = \gamma Q H \tag{6}$$

where:

Q=Flowrate $[\frac{m^3}{s}] or [gpm]$

H=Head $[m] or [ft]$

γ=Specific weight $\frac{N}{m^3} or \frac{lb}{ft^3}$

The brake horsepower or input to a pump is greater than the hydraulic horsepower or output due to the mechanical and hydraulic losses incurred in the pump. Therefore the pump efficiency is the ratio of these two values. (Efficiency value is only expressed for mechanical point, electrical power and efficiency from generator are not taken into account)

$$\eta = \frac{whp}{bhp} \tag{7}$$

where:

η=Efficiency

whp=Hydraulic pump power [W]

bhp=Brake horsepower [W]

Specific speed. Specific speed N_s is a non-dimensional design index used to classify pump impellers as to their type and proportions. It is defined as the speed in revolutions per minute at which a geometrically similar impeller would operate if it were of such a size as to deliver one gallon per minute against one foot head.

The understanding of this definition is of design engineering significance only. Specific speed should be thought of only as an index used to predict certain pump characteristics. (GOULDS, 2009). Figure 6, shows a relationship between specific speed and the most suitable type of impeller for given speed. In simulation section this concept is required to perform a calculation for turbine operation conditions

$$N_s = \frac{NQ^{\frac{1}{2}}}{H^{\frac{3}{4}}} \tag{8}$$

where:

N_s=Suction speed (Dimensionless)

N=Pump shaft rotational speed $[rpm]$

Q=Flowrate at best efficiency point $[\frac{m^3}{s}]or[gpm]$

H=Head at best efficiency point $[m]or[ft]$

Figure 6: Impeller Design vs. Suction Speed

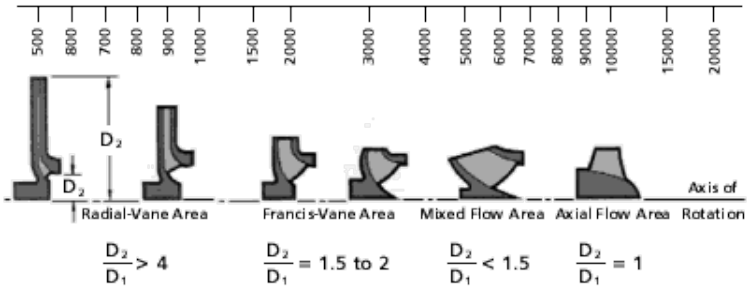

(GOULDS, 2009)

Centrifugal pump characteristic curve. A typical characteristic curve shows the total dynamic head, input power, efficiency, and Net Positive Suction Head (NPSH) all plotted over the capacity range of the pump. NPSH shows the difference between

pressure at a certain point of the pump and the vapor pressure of the fluid involved in the process. This parameter is useful for predicting cavitation. Relating to the pump characteristic curve, for a radial flow pump the head curve is relatively flat and with head decreasing gradually as the flow increases while input power increases gradually over the flow range with the maximum normally at the point of maximum flow. Most turbine pumps are also in this same range up to maximum flow, depending upon their specific speeds.(GOULDS, 2009)

Figure 7: Centrifugal pump characteristic curve

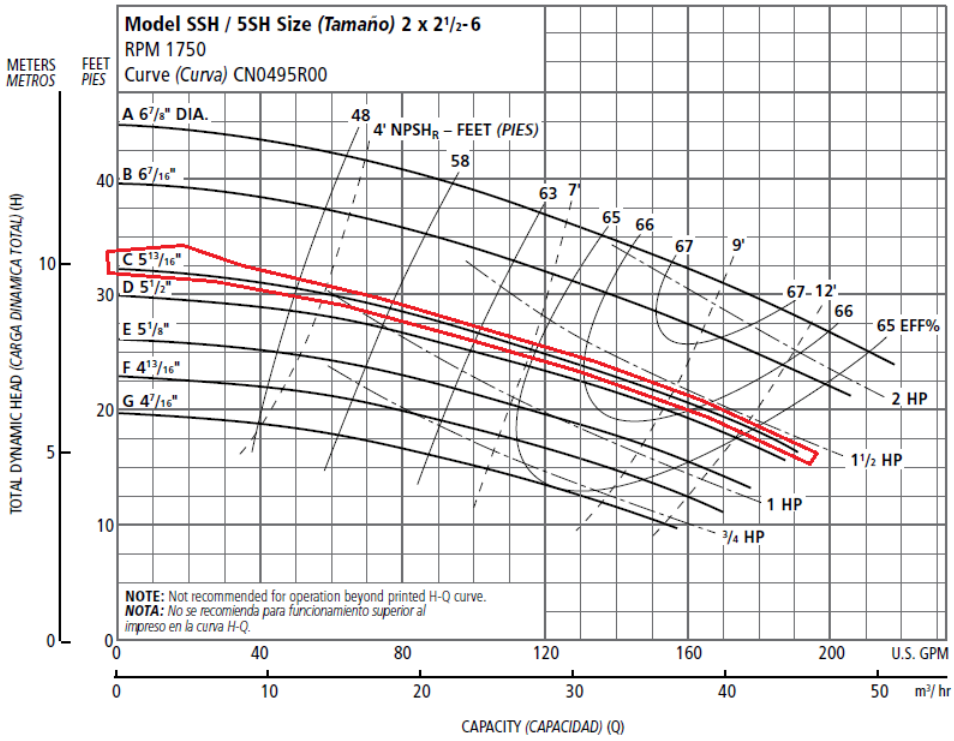

Optional Impeller, *Impulsor Opcional*		
Impeller Code, *Código del Impulsor*	**Dia., *Diá.***	**Standard HP Rating, *Estándar HP Potencia***
A	6 7/8"	2
B	6 7/16	2
C	5 13/16	1 1/2
D	5 1/2	1 1/2
E	5 1/8	1
F	4 13/16	1
G	4 7/16	3/4

NOTE: Pump will pass a sphere to 5/32" diameter.

NOTA: *La bomba pasará una esfera a 5/32" diámetro.*

(GOULDS, 2009)

Pump performance curve relates head and flow delivered by the pump. Inside the curve plot, the best efficiency point (BEP) which is where head and Flow rate coin-

cide with the maximum efficieny of the machine, is located at a particular flow rate value depending on pump characteristics such as type and size. BEP is typically around 40% to 80% of efficiency.(WILLIAMS, 2003)

When no efficiency data is available, the use of input power against flow rate chart allows one to calculate BEP values in the following manner:

$$\eta = \frac{H_p Q_p \gamma}{P_p} \cdot 100 \tag{9}$$

where:

η=Efficiency

P_p=Pump input power $[W]$

Q_p=Flowrate at BEP $[\frac{m^3}{s}] or [gpm]$

H_p=Head at BEP $[m] or [ft]$

In the case of limited data, one approximation for the BEP conditions can be made with the following equations, established by Williams:

$$Q_p = 0.75 Q_{max} \tag{10}$$

$$H_p = 0.75 H_{max} \tag{11}$$

Whether the pump has an integrated motor, the power curve is related to electrical power consumption and can be calculated as follows:

$$P_p = P_{elec} \frac{\eta_{motor}(\%)}{100} \tag{12}$$

where:

η=Efficiency

P_p=Pump input power $[W]$

Q_p=Flowrate at BEP $[\frac{m^3}{s}]or[gpm]$

H_p=Head at BEP $[m]or[ft]$

4.2 Centrifugal Pump as Turbine Fundamentals.

Focused in the application of pumps as turbines for micro-power generation, the following theoretical concepts will afford the main features of the project objectives and will leave out some concepts from pump and turbine theory.

4.2.1 **Operation.**

Operating mode in a centrifugal pump is established by constant flow rate, head and rotation velocity so they are designed for a specific work stage. As said before, on ideal conditions this point is called BEP (Best Efficiency Point). On the other hand, operating mode of a turbine differs from pump having variable flow rates and head as well as devices to regulate flow rate whereas water variations exist (i.e not regular conditions of flow rate).

While operating in pump mode and inside BEP with nominal rotational velocity where the flow shows an optimum behavior, head or pressure at oulet are reduced due to hydraulic losses (i.e friction and volumetric losses). Operation of the pump in turbine mode and with the same velocity as working on pump mode, the inlet pressure head should be increased up to equivalent hydraulic losses in order to achieve the BEP. Efficiency for the pump operating in turbine mode can differ significantly due to several variation between losses' parameters such as volute casing shape and design, number of vanes, vane angles, etc. (AUDISIO, 2009) From now on, the word PAT will be used to describe the pump operating in reverse mode (Pump as Turbine)

Reverse operation of standard pumps provides advantages over conventional turbines for micro-hydro power generation:

- Wide range of heads and flows
- Available in a large number of standard sizes
- Low cost
- Spare parts availability
- Easy installation

The main limitation of PAT is that the range of flow rates is less compared with conventional turbines. When using PAT instead of conventional turbines, a direct shaft arrangement gives even more advantages over turbines and belt driven configurations. Some of these advantages are:

- Low friction energy in shaft
- Lower cost
- Less maintenance

Using combined pump-motor units is recommended for electricity production within micro-hydro schemes, where the simplest installation is a requirement. Disadvantages of integral units can be reduction in range of flow rates because of turbine and generator speed relationship and limited choice of generators for particular PAT.

4.2.2 **Pump and turbine differences.** Hydrodynamic theory for both machines is similar, however the flow behavior shows differences between pump and turbine design.

For both machines, pressure head changes in opposite way with flow rate. Total head for turbines decreases with flow rate increment while for pumps the total head increases proportionally to flow rate increment.

Relating to design, in a pump the kinetic energy given to the fluid must be transformed fully or partially in pressure energy by a deceleration process between impeller eye and volute casing. Inside the deceleration process, boundary layer phenomena of vanes has influence in frictional losses and vortex formation. The design of the vanes has been developed in order to minimize these kind of effects and increase pump efficiency. In turbines, as the flow is accelerated there exist more turbulence behavior but inside rotor passages the frictional losses are reduced so the overall efficiency is better as regarding to pumps.(AUDISIO, 2009)

Performance in pump and turbine mode differs according to flow rate, power and efficiency. Performance comparison can be seen on table 1

Table 1: Pump Turbine comparison

	Flow rate	Power	Efficiency
Pump	Lessen while head increases up to a null value for maximum head	Demands minimal power for the maximal head	Efficiency increases along with flow from zero up to a maximal point. From here forward, decreases while flow continue with its increment
Turbine	Continuous increment while head increases	Flow must exceed a minimal value (vacuum flow rate) for operation.BEP is higher than pump mode BEP therefore torque in shaft is greater	Efficiency increases from zero and vacuum flow rate up to a maximal point and then decreasing slowly as the flow rate increases

(AUDISIO, 2009)

PAT performance curves. For the pump operating as turbine, the flow increases with increasing head. The operating point of the turbine is found by plotting together the PAT (Head vs flow) curve and the site curve (head vs flow available at site). The site curve is made by finding the available head at the turbine (vertical height between the intake from stream and turbine outlet, less frictional head loss in the penstock) (WILLIAMS, 2003). Turbine's speed will vary regarding to the load which is being subjected, so there exists a different head-flow curve for each speed. If a load, higher than design load is involved, speed reduces. The case of centrifugal pump operating as turbine causes the flow rate to have a meager increment. Oppositely, when the load is reduced, speed increases until the point where a condition of no load exists, in which speed increases up to maximum, this is known as *runaway* In

figure 8, the BEP point can be seen where both head and flow rate for the turbine H_t and Q_t intersect as well as the limit for the PAT operation. This limit point is where the PAT reaches its runaway velocity, being harmful for the shaft and motor to continue the operation.

Figure 8: Centrifugal pump as Turbine characteristic curve

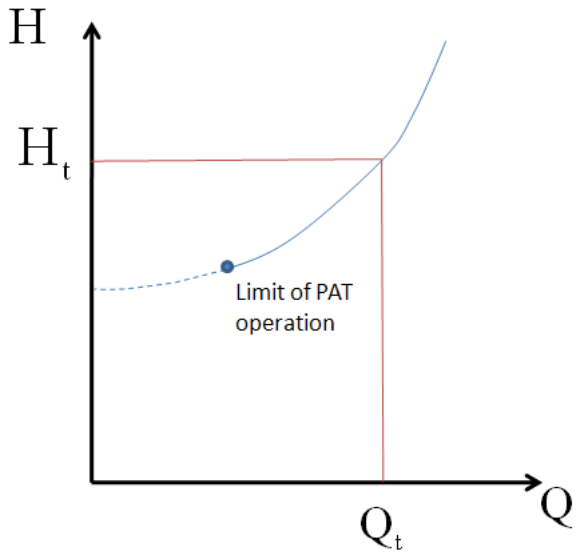

(WILLIAMS, 2003)

Affinity laws and dimensional analysis in turbomachines. The majority of pumps operate at different velocity to obtain several values for capacity Q. Also the volute casing can be suited to different impeller diameters. To guarantee the understanding of changes in capacity, head and power as well as to be able to scale hydraulic machines, a list of relations called *Affinity laws* are defined. These laws are used to calculate volume capacity, head or power consumption in centrifugal pumps when changing speed or impeller diameters. Subscripts 1 and 2 are related to different pumps.

1. Changes in velocity

   - Capacity changes in direct manner with velocity

$$\frac{Q_1}{Q_2} = \frac{N_1}{N_2} \tag{13}$$

   Q=Flowrate (Capacity)$[\frac{m^3}{s}]or[gpm]$

   N=Rotational speed $[rpm]$

   H=Head $[m]or[ft]$

   P=Pump required power $[W]$

   - Total head changes with the square of the velocity

$$\frac{H_1}{H_2} = \left(\frac{N_1}{N_2}\right)^2 \tag{14}$$

   - Power required for the pump changes with the cubic of the velocity

$$\frac{P_1}{P_2} = \left(\frac{N_1}{N_2}\right)^3 \tag{15}$$

2. Changes in impeller diameter

   - Capacity changes in direct manner with the diameter of impeller

$$\frac{Q_1}{Q_2} = \frac{D_1}{D_2} \tag{16}$$

   Q=Flowrate (Capacity)$[\frac{m^3}{s}]or[gpm]$

   N=Rotational speed $[rpm]$

   H=Head $[m]or[ft]$

   P=Pump required power $[W]$

D=Diameter of impeller $[m]$

- Total head changes with the square of the diameter of impeller

$$\frac{H_1}{H_2} = \left(\frac{D_1}{D_2}\right)^2 \tag{17}$$

- Power required for the pump changes with the cubic of the diameter of impeller

$$\frac{P_1}{P_2} = \left(\frac{D_1}{D_2}\right)^3 \tag{18}$$

Efficiency is kept constant for changes in velocity and small variation of impeller diameter. (MOTT, 2006)

The concept of affinity laws is in close relationship with dimensional analysis performed to turbomachines in order to carry on good modeling of machines with similar characteristics. Because the great size and complexity of turbomachines, modeling such machines becomes a common practice to make generalizations and predictions of parameters like velocity, flow rate or energy in terms of head. In machines in which no important considerations of heat transfer occur, the power, P, required or delivered by turbomachinery with similar geometry will depend on:

- Characteristic length of runner or impeller diameter: D
- Rotative speed: N
- Volume flowrate: Q
- Added or subtracted energy: H
- Fluid characteristics: viscosity μ and density ρ

Relationship between variables and Buckingham-Π analysis define dimensionless coefficients for Power, Capacity and Head.

$$\Pi = \frac{P}{\rho N^3 D^5} \text{(Power coefficient)} \tag{19}$$

$$\Phi = \frac{Q}{N D^3} \text{(Flow coefficient)} \tag{20}$$

$$\Psi = \frac{H}{N^2 D^2} \text{(Head coefficient)} \tag{21}$$

Dimensionless parameters are useful for experimental testing and authors like (RAWAL and KSHIRSAGAR, 2007) and (DERAKHSHAN and NOURBAKHSH, 2008) had implemented these, acquiring good approach and results that will be presented and revised in a further step of the present project.

Considerations for electrical power generation. Electrical power generation is beyond the scope of this project. Nevertheless a brief description of the manner, the electrical power will be manipulated is described in the next paragraph. Regarding to electrical power generation, synchronous generators are commonly used to produce AC electricity when no grid supply is available. The great disadvantages of this kind of machines are the high cost and the short life of machines operating with petrol or diesel at continuous operation. For these reasons, induction motors used as generators have been recently installed on micro-hydro power schemes, showing more reliable behavior than synchronous generators and becoming a inexpensive option for electrical power production. (SMITH, 2008) The project will deal with a induction motor used as generator with direct drive configuration because it becomes economically viable and availability in local market is guaranteed.

4.3 **Computational Fluid Dynamics (CFD)**

4.3.1 **Description.** Computational Fluid Dynamics is the analysis of systems involving flows, heat transfer and related phenomena such as chemical reactions by means of computer-based simulation (VEERSTEG and MALALASEKERA, 1995). CFD is based on numerical methods for PDE (Partial Differential Equations) solution in order to achieve the values of variables used within the simulation in any moment of time and in any part of the domain in question. Modern uses of this computational tool reflect the importance in analysis support for technical equipment design and research. Application fields for CFD methods extent to systems where fluids are involved.

- Aerodynamics in planes and vehicles
- Hydrodynamics
- Internal combustion engines
- Turbomachinery
- Electrical and electronic engineering
- Environmental engineering
- Biomedical engineering (VEERSTEG and MALALASEKERA, 1995)

4.3.2 **Background and development in hydraulic machines** CFD was developed after the computational advances for integrating mathematical knowledge of TFD (Theoretical Fluid Dynamics). The pioneers in CFD techniques were research centers and laboratories. Nowadays there exists specialized software for CFD that

makes flexible studies regarding the scenario which the analysis will be performed as well as fast, reliable and graphical results.

Some advantages of CFD in flow system analysis are:

- Time and Money reduction for new product development and analysis
- Ability to perform analysis in systems where it is hard or even impossible to execute secure controlled experiments.
- No limits on results visualization (VEERSTEG and MALALASEKERA, 1995)

One of the most important advantages is the money saving, despite it has important costs in relation to computational time and high computing; the cost is less compared to physical experiment in wind tunnels or hard control environments.

Commercial CFD codes are meant to discretize and solve the differential Navier–Stokes equations for continuity. These equations were stated by Claude Louis Navier and George Gabriel Stokes in 1822. These equations arise from applying Newton's second law to fluid motion, together with the assumption that the fluid stress is the sum of a diffusing viscous term (proportional to the gradient of velocity), plus a pressure term.

The Navier-Stokes equations considered for the present case are the mass continuity equation and the incompressible flow formulation Adopting the incompressible flow assumption where density becomes a constant, and neglecting temperature effects, continuity equation is:

$$\nabla \cdot \mathbf{v} = 0 \tag{22}$$

The incompressible form combines nonlinear terms for convective acceleration (caused

by changes in velocity over position, i.e accelerated flow inside impeller's ducts), divergence of stress, expressed as the diffusive term because of viscosity effects and other forces such as centrifugal force or gravity.

$$\overbrace{\rho(\underbrace{\frac{\partial \mathbf{v}}{\partial t}}_{\substack{\text{Unsteady}\\ \text{acceleration}}} + \underbrace{\mathbf{v}\cdot\nabla\mathbf{v}}_{\substack{\text{Convective}\\ \text{acceleration}}})}^{\text{Inertia (per volume)}} = \overbrace{\underbrace{-\nabla p}_{\substack{\text{Pressure}\\ \text{gradient}}} + \underbrace{\mu\nabla^2\mathbf{v}}_{\text{Viscosity}}}^{\text{Divergence of stress}} + \underbrace{\mathbf{f}}_{\substack{\text{Other}\\ \text{body}\\ \text{forces}}} \tag{23}$$

Regarding to hydraulic machines it is important to settle some strong issues about the development of several methods to come up with solutions for this kind of machines

In the 1970s, aerodynamics and structural mechanics had improved numerical methods such as finite difference and finite element methods. The challenge at the time was to introduce these new numerical methods into the traditional world of hydraulic turbomachines with its emphasis on experimental development

An overall explanation of numerical methods applications is given by meaning of some examples and most important features of turbomachinery development

The first success of CFD in modeling turbine flows came after the change of simple geometries treatment into complex geometries with good accuracy

The first step of using FEM for a CFD application was just to program a post processing tool that allowed velocity components (and static pressure) to be calculated over the nodal points of a bulb turbine's grid and to formulate proper boundary conditions(KECK and SICK, 2008). As seen nowadays, the most critical task in order to get useful results is the specification of boundary conditions. Evolution took the engineers to perform analysis with mass and momentum and solve the Reynolds Av-

eraged Navier Stokes Equations (RANS) through commercial codes like ASC, CFX and nowadays Ansys CFX. The steady state RANS model gives a more comprehensive approach to viscous and turbulence effects, loss analysis, boundary layer effects in turbine components and decelerated flow analysis.

Despite in the middle of the 80s mathematical models involved time dependent interaction between rotating and stationary components until decades later it could be possible to represent these components in the solving of RANS. Validation of the computational method and parameters such as the computational domain and boundary conditions, the computational grid, discretization scheme and turbulence model has become a significant task. (KECK and SICK, 2008)

From the 90s the importance of new designs and optimization improved a lot more the methods as well as the economical factor because a full model test was in the same order of a medium size new runner.

Another important development is given by recent studies of unsteady flow and its effects on structural components caused by dynamic loads. For example in a francis turbine three major items regarding to dynamic load can be presented.

- Structural damage caused by draft tube vortex
- Structural damage caused by Von Karman's vortex shedding at trailing edge of vanes
- Stationary (guide vanes) and rotating (runner blades) interaction.

The structured mesh for a Francis turbine can be seen in figure 9

Figure 9: Francis turbine runner mesh

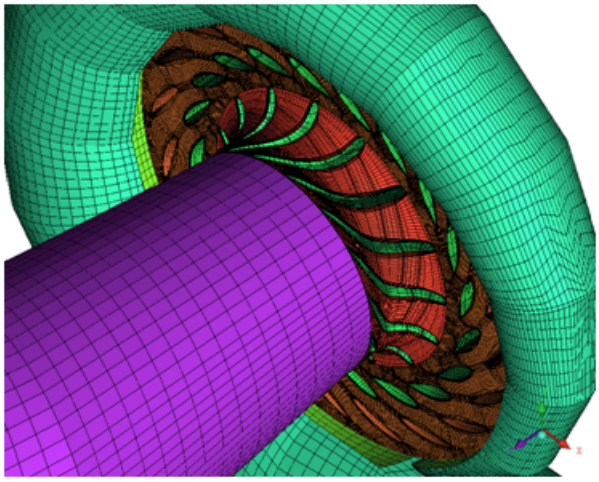

(ORREGO, 2009)

Good prediction of draft tube vortex can be achieved with good turbulence modeling and methods such as Reynold stress model or Large Eddy simulations. Mostly methods of two equations (k-epsilon and others) can not handle strongly curved flow paths due to the assumption of flow isometry (KECK and SICK, 2008). Hence a good practice of method selection is always an important task to complete by the engineer. Nowadays research and use of CFD is intended to these kinds of analysis as well as multhiphysics and fluid-solid interaction

4.3.3 **General CFD process** CFD process is treated in the same way for any problem involving fluids. There are established stages that must be completed in order to have complete control of the simulation and preserve order between variables and physical parameters. Good tracking of the CFD process is fundamental to keep oriented in the solution of the problem. If one of the stages is not successfully fulfilled, problems in the following stage may appear. Process is seen in figure 10.

Figure 10: CFD General Process

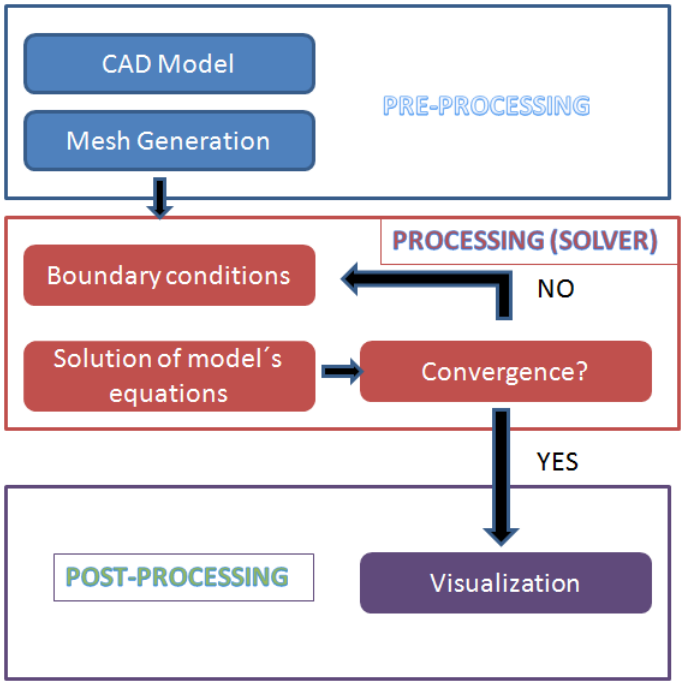

Description of stages for the CFD process are presented:

1. Pre-processing First interaction between the user and the intended project to develop. Inside the pre-processing there are some tasks to be fulfilled:

    - CAD model creation for realistic representation of the physical problem
    - Mesh generation and refinement according the simulation orientation and features of the problem taking account further consideration for Boundary condition definition. The mesh can be defined as *structured mesh*, characterized by regular connectivity that can be expressed as a two or three dimensional array. This restricts the element choices to quadrilaterals in 2D or hexahedra in 3D. An *Unstructured mesh* is characterized by irregular connectivity is not readily expressed as a two or three dimensional array in computer memory. This allows for any possible element that a solver

might be able to use and a *Hybrid mesh* is a mesh that contains structured portions and unstructured portions. (CFDOnline, 2009) Example of structured and unstructured meshes can be seen in figure 11.

Figure 11: Structured and unstructured Meshes

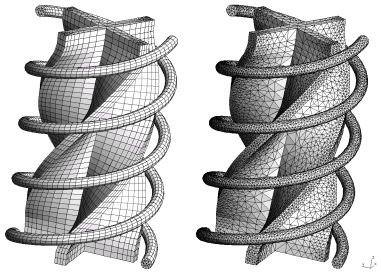

(GMSH,2010)

- Physical model definition, boundary conditions, environmental and fluid properties as well as input parameters for the solver. These items should define accurate approximation to physical phenomena achieving correct simulation results

2. Processing Solution of the PDE using numerical iterative methods for the selected physical model by means of applying mass and moment conservation laws to control volumes within the defined domain. The calculation for desired variables should be preserved between defined ranges of convergence parameters.

3. Post-processing Post-processing allows the user to study results and give correct interpretation to the behavior of desired variables in a graphical environment.

4.3.4 **Numerical Methods for solving turbulence.** The great amount of methods for simulating turbulence had improved the CFD study by developing mathematical models that vary in complexity and approach to the solution of RANS (Reynolds Averaged Navier Stokes) equations , DNS (Direct Numerical Simulation) and LES (Large Eddy Simulation). Because of the complexity of some models and diverse application fields they can be fitted in, these models will not be explained. Further research inside this project will determine which model is suitable for carrying out the simulation taking into account, complexity, system requirements and profit–time relationship

The solutions of turbulent model equations are based on iterative calculations of required valuables within correct measurement of convergence parameters like (RMS, MAX, etc) and definition of boundary conditions.These convergence parameters are explained in chapter 7

Depending on the case of study, the addition of other equations to be solved together with the Navier-Stokes Equations is required. Some examples:

- Turbulence model equations
- Heat transfer equations
- Multiphase equations

In addition, the solution of these equations can be achieved by different methods, being the most popular the following three:

1. Finite Difference Method (FDM). The domain is represented by a set of points and only at those points the results are obtained. The discretization of the

equation begins with conservation equation in differential form and then by substituting differential operators with finite differences (truncated Taylor series expansions) obtaining an algebraic approximation of the equation. Applying the approximate equation to each point results in a system of algebraic equations.

This method has advantages in handling simple geometries discretization but its behavior with well curved boundaries and complex geometries is not precise. Also as based on derivative approximation is less accurate than Finite Element (FEM) and Finite Volume(FVM) methods.

2. Finite Element Method (FEM). The domain is divided in a set of elements where results are obtained at the nodes on the corners or along the edges of the elements. The conservation equation is first expressed using the Method of Weighted Residuals or Galerkin, and dependent variables are approximated by a series of interpolation polynomials (shape functions). Shape functions, multiplied by weight functions, are integrated over each element and these integrals are minimized in order to satisfy the governing equations. The small systems of equations obtained in each element are assembled into a large global system of algebraic equations.

   Regarding to advantages it can be stated that for linear PDEs, solution often can be proven mathematically to be exact at the nodes. This method is the best for complex geometries and local grid refinement being the method of choice in solid mechanics. The FEM method is usually less efficient than FDM or FVM in heat and flow simulations and intermediate results physically after discretization are hard to interpret.(LANGE)

3. Finite Volume Method (FVM). The domain is divided in a set of control volumes (CV) and results are obtained at the center of each CV. Algebraic approxima-

tion of the equation is obtained by using linear interpolation functions that are integrated over each CV, producing a balance of fluxes in and out of the CV. The approximate balance (conservation) equations in each CV result in a system of algebraic equations. Advantages show that terms in the discretized formulation have direct physical interpretation and the method is usually the most efficient for heat and flow simulations. In the other hand is only suitable for flux calculations (not solid mechanics) and does not converge as well as FEM for highly nonlinear problems. (LANGE)

In practical CFD commercial codes, the implementation of the finite volume method is widely used. For the simulation of the pump, a research and selection of an adequate turbulence model as well as good boundary conditions definition is needed. For example a previous study of this kind of pump operation system denoted as PAT (Pump as Turbine) has been made by (RAWAL and KSHIRSAGAR, 2007). Inside this research the authors had used the k-epsilon turbulent model because it is considered to achieve good accuracy and stability, and implemented in most of the CFD codes because it is numerically well supported and with established predictive capability. Despite the use of this procedure, some effects of the PAT behavior could not be simulated because of limitations and external disturbances in the system like components losses. Results and predictions for numerical simulation will be achieved for the BEP (Best Efficiency Point) without taking into account losses of the system. Nevertheless a further study with improved quality meshes and superior turbulence model will provide a better approximation.

4.3.5 **Ansys CFX Software.** Ansys CFX software is a high level program for general purpose in CFD analysis, which has been used for more than twenty years.

Flexibility offered by the software permit in addition to a good simulation approach, adequate, simple and focused parameter behavior and results.

Ansys CFX will be used to perform the simulation and analysis of the pump.Also an additional package of the software can be used for the meshing, ICEM CFD. The election of this CFD software package guarantees support because is worldwide known, has a comprehensive environment for the user and can handle the whole simulation from the very first considerations of pre processing to the results visualization and analysis. Despite there exist documentation about other CFD software, CFX is considered by the author of the project as the best one due to the complete integration of the process from pre to post and compatibility of files and solving parameters.

5 DIGITIZING OF CAD MODELS

The process of duplicating an existing part, subassembly or product, without drawings, documentation, or a computer model, is known as reverse engineering (RAJA and FERNANDES, 2008). This method will be used for the project. The first part of the project was to acquire CAD (Computer Aided Design) models of the provided pump. The application of two techniques for digitizing allowed to create and edit the geometry of the pump inside a CAD software in order to move forward through CFD process. The acquisition of CAD models was done with Laser Digitizing technique and articulated-arm digitizing. The Handyscan digitizer with commercial VXscan software and MicroScribe 3DX arm were used following a procedure explained as follows.

5.1 **Part digitizing**

Each one of the techniques to obtain the geometry of the parts required special configuration aimed to obtain good quality and correct data for CAD processing.

5.1.1 **Handyscan** Laser digitizing technique involves the acquisition of geometry through a device able to shoot laser beams and get information after reflection in the surfaces of the part to be scanned. Handyscan is a commercial 3D scanning device that consist of a handheld laser and processing software.

To set up the part, it is needed to stick up *reflective targets* following a triangular path along the part and focusing on details (see figure 12). The triangular distribution

guarantees continuity of signal between targets in order to generate real time rendering and position for the beam. Therefore the brightness and reflective sections of the part are covered by spray-painting (this is done because the targets are the only elements that must reflect the laser for image capture). Once the part is painted, it is important to make it stable and avoid movements of the part that might result in poor acquisition of surfaces and further trouble with reconstruction within the software.

Figure 12: Triangular path

The procedure to continue after good position of the part is the calibration of the laser scanner. This is performed inside VXscan software by the measurement of laser beam intensity in a recorded section of the part executed in a previous scan. Calibration of the scanner is necessary to capture better shapes of the part.

Once everything is set up the process begin with correct aiming of part features and slowly movement of the digitizer assuring full acquisition of surfaces. The reflection of the laser beam is picked up by two stereoscopic digital cameras and then processed to obtain real-time rendering,allowing the user to control which section of the part is being scanned and performing corrections in the way. The duration of digitizing process is up to the scan quality and limitations found by the user. The volute casing and cover parts were digitized following the procedure and obtaining separated *stl* files with faceted mesh data for post processing in CAD/CAM software. The configuration for digitizing process is shown on figure 13

Figure 13: Handyscan digitizing process configuration

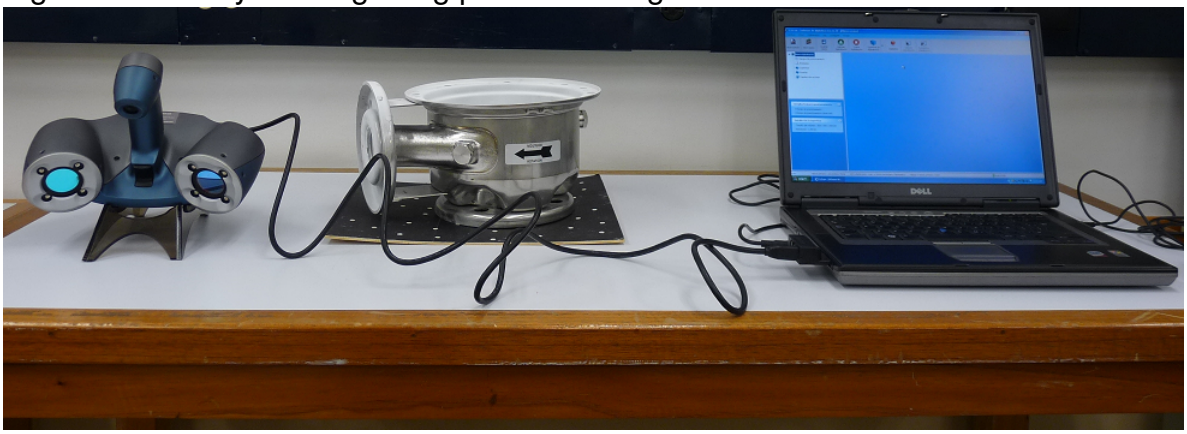

5.1.2 **MicroScribe 3DX.** The implemented technique in the MicroScribe device is the arm-digitizing which consist in the acquisition of points from the real part by positioning the arm's stylus on each marked point in the surface and pressing a pedal to save the point in a CAD software or a text file as a point list.

For data acquisition with the MicroScribe 3DX, the position of points on part's surfaces is only needed. Either targets or painted points can be used, however consistent geometry is required. In this case the use of the MicroScribe digitizer was limited to the outlet of the volute casing (inlet condition for Turbine operation) and impeller, due to the difficulties of digitizing with the Handyscan device. Following the considerations taken with the Handyscan, the part must be fixed and the digitizer calibrated. Calibration was performed inside Rhinoceros 4.0 software and installed MicroScribe plug in. In figure 14, the used configuration is shown.

Figure 14: MicroScribe 3DX digitizing process configuration

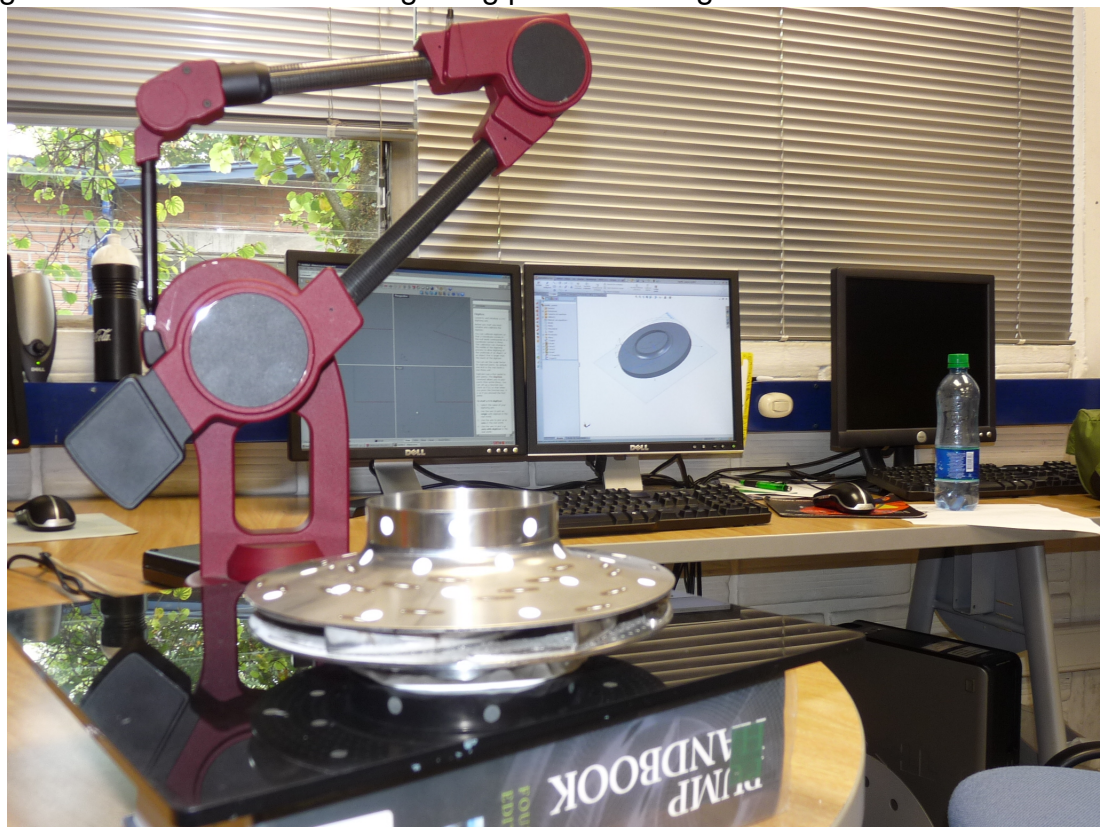

The process with the MicroScribe 3DX digitizer requires more time than the process with the Handyscan because careful inspection of the part and geometry distinction should be carried out before beginning. The digitizer is plugged, installed and recognized by Rhinoceros plug in. Calibration of the arm is done by clicking the origin of coordinate system for the part and defining X and Y axis with arm's stylus. Once everything is set up, digitizing process start with positioning of the stylus on each of one of the marks plotted in the part and clicking by pedal or keyboard to capture the point. After completing the whole model, a point cloud can be seen inside Rhinoceros windows. The point cloud could have been processed inside Rhinoceros, but due to technical resources and author's ability and experience working with Solidworks, text file export was preferred.

5.2 **CAD models post-processing**

Talking about digitizing, post-processing of obtained model data is doubtless the most time-demanding and hard task to perform because complexity of shapes, noise and erratic data appear regularly. Reconstruction of surfaces is a demanding task according to the obtained quality from digitizing process. In the present case, the digitized model parts (STL files) were loaded in Rhinoceros and cleaned using tools for holes repair and point suppression. An example of Rhinoceros feature for noise removal can be seen in figure 15

Figure 15: Volute before and after noise removal (Rhinoceros)

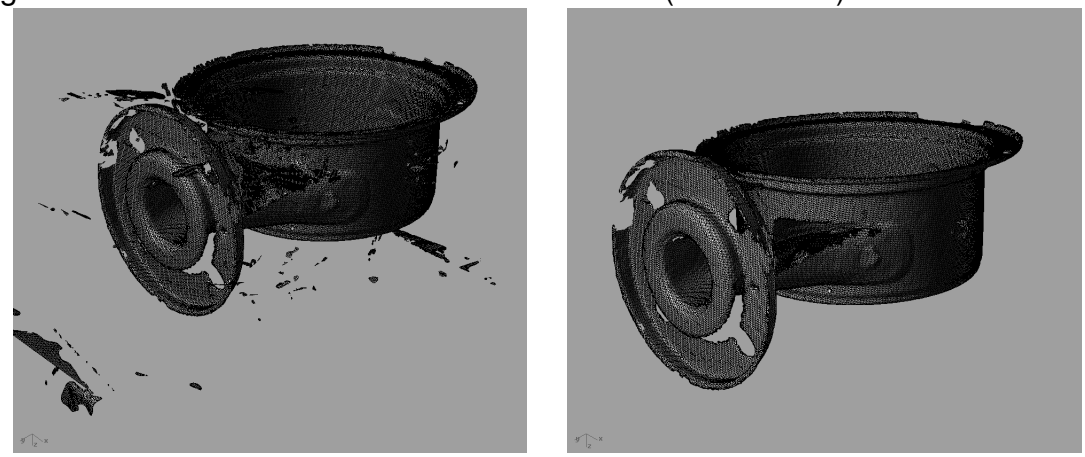

(a) Before (b) After

5.2.1 **Volute lid.** The first loaded model was the lid that connects the shaft and the impeller presenting no more than 30% of point noise after digitizing. The noise was eliminated by point suppression and small holes presented in the STL mesh, refilled with special mesh editing tool from Rhinoceros. Digitizing of lid presented no major trouble so the reconstruction was almost done inside the VXscan software. This part has special curvature features that involve the behavior of the flow as it

enters the volute casing.

Once repaired, the model was exported as point cloud file to Solidworks for further processing (see figure 16). Despite there are such great tools for surface reconstruction within Rhinoceros, gained experience in Solidworks allows the author to ease the reconstruction process saving valuable time for the project without sacrificing good quality. The file is then loaded into Solidworks and configured with the ScanTo3D module. This process is guided through few steps allowing one to perform another surface analysis in order to refill holes, clean the model and smooth surfaces.

Figure 16: Scan To 3D lid reconstruction

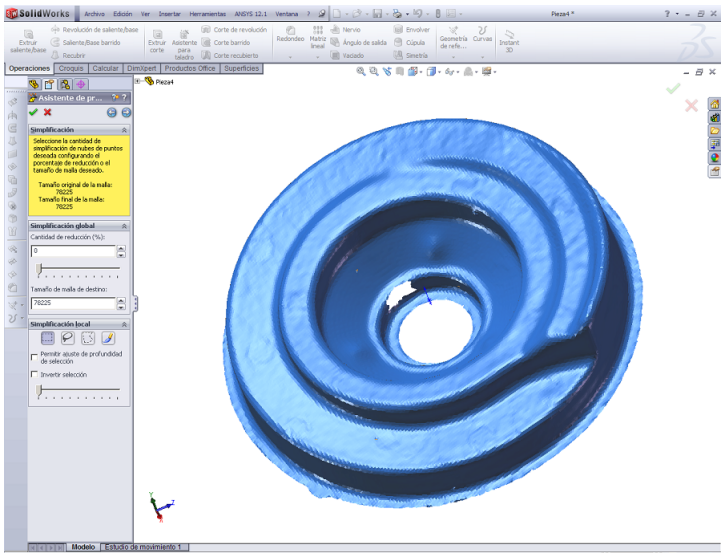

In figure 17 the real part can be compared with the digitized model.

5.2.2 **Volute casing.** The described process in the lid section was used for volute casing part in the same manner, but spending more time according to a lower digitizing quality due to the volume of the digitized part and its geometry. In this case there was more noise than the lid, demanding a more focused task inside both Rhinoceros

Figure 17: Volute lid geometry

(a) Real (b) Scanned

and Solidworks software. After processing surfaces in Solidworks the next step was to convert them to solids by giving them thickness and then assembling the volute casing with the lid. the result can be seen in figure 18

Figure 18: Volute (Solidworks)

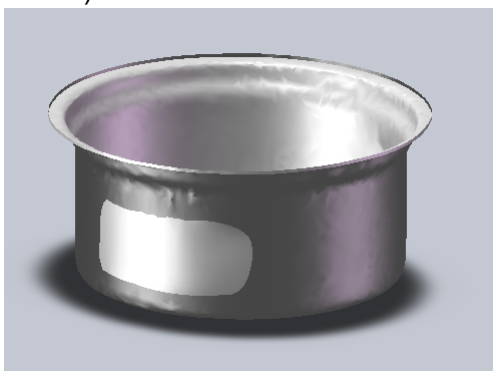

The goal of the digitizing post process is to obtain the domain in which the analysis of the PAT is going to be performed. In other words the domain is the space where the flow will be passing through from Inlet to Outlet. In order to acquire this domain of fluid it was necessary to operate solids (volute casing, volute lid and impeller) by a Boolean difference within Solidworks's combine feature. In figure 19 one can see the result of the boolean operation and the space where the impeller is assembled.

Figure 19: Complete Volute in Solidworks

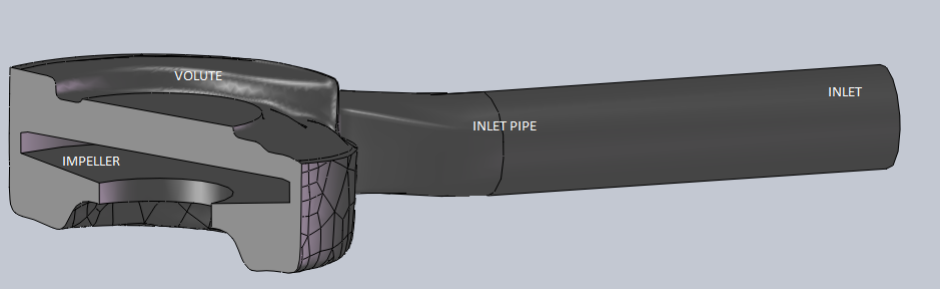

In the meshing section the domain division will be explained.

5.2.3 **Inlet** PAT's inlet was digitized in a different way using the MicroScribe 3DX digitizer. The inlet was set up before point acquisition placing the part on a solid surface and chosing the origin of the part in the software. This part is shown on figure 20

Figure 20: Inlet digitizing process with MicroScribe arm

Two contours were digitized, the intake from the penstock and the volute casing-inlet interaction, as well as a curve throughout the inlet used as a guide for both contours for further Solidworks surface creation. Both countours and the path were saved in *.txt* files and loaded into Solidworks with the import curve feature. After having the

geometry inside Solidworks the next step was to create a lofted surface between countours guided by the path line. In order to complete the solid, inlet and volute interaction surfaces were created and knitted. The result can be seen in figure 21

Figure 21: Inlet (Solidworks)

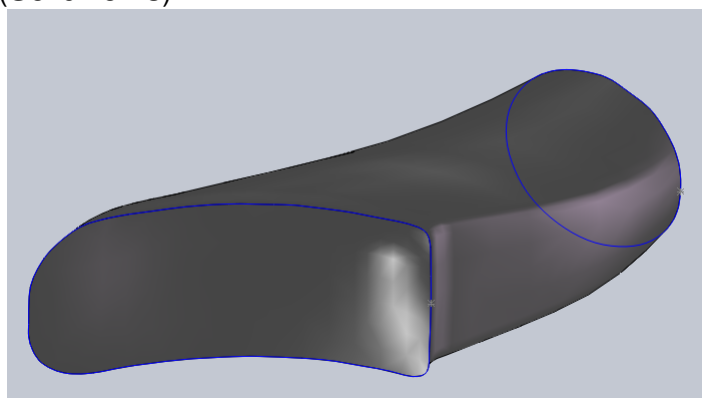

5.2.4 **Impeller.** Digitizing of impeller was performed with the MicroScribe arm by taking points from both sides of one vane. The profile for both leading and trailing edges of the vane were imported to Solidworks and used as contours for a lofted operation. The trajectory for the operation was also digitized in the surface in contact with the hub. One vane was created after the operation and a circular pattern applied to generate the whole impeller and check whether interferences existed.After checking the geometry only two vanes are needed to generate one domain duct where the fluid is going to cross. The creation of the duct involved operations with surfaces. The idea was to generate the mesh around the shape of the vane in order to achieve near wall detail. Figure 22 shows the geometry for the duct and the leading and trailing edges of one vane.

Figure 22: Impeller (Solidworks)

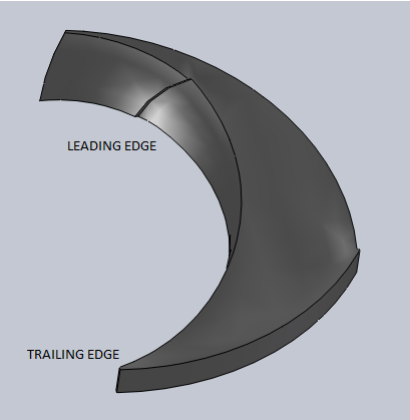

5.2.5 **PAT Discharge pipe.** Despite there exists a discharge pipe in the simulation it was not required for digitizing because it is not a complex part and can be modeled easily after having all the geometry of the impeller. This part was modeled after having the whole impeller geometry by taking the geometry of the vane at suction eye and applying a revolution operation. The length was considered as 5 times the diameter of the outlet to assure good development of the flow. In figure 23 the geometry of the discharge pipe can be seen as well as its regions.

Figure 23: PAT discharge pipe(Solidworks)

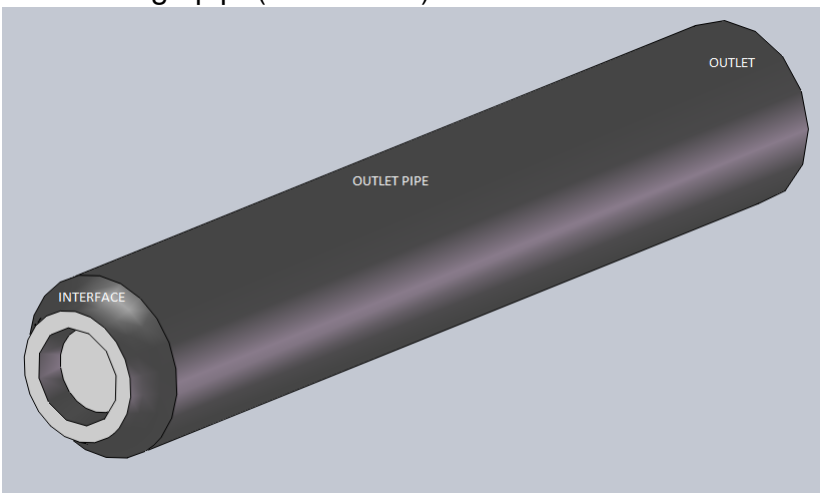

When all parts were digitized, they were assembled together and checked for interferences encountering no problems during the reconstruction of the geometry. Figure 24 shows the assembly of all the parts and the names they get for better reference in the meshing process. This names are: Part A for the volute, B for the impeller, and C for the discharge pipe.

Figure 24: Complete geometry(Solidworks)

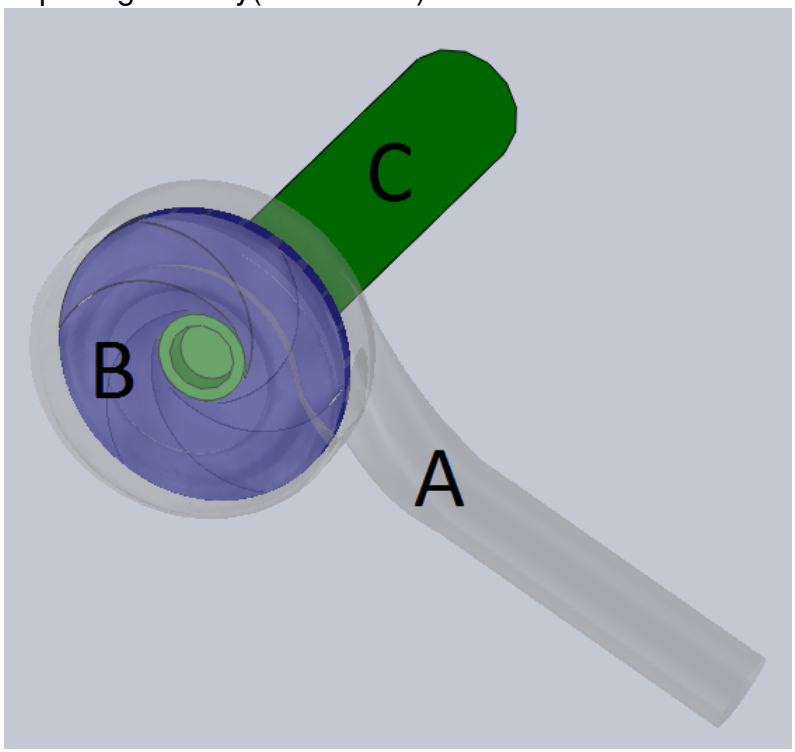

5.3 **Geometry and quality check of parts**

There exist an obligation to compare the digitized model with real measurements from pump's parts. Because of geometrical manipulation for correct adaptation of parts within the software, parts might not match up completely. Nevertheless, general shape and consistency of geometrical entities is guaranteed. Dimensions of parts A and B are shown in figures 25 and 26 respectively, and then a table compar-

ing main dimensions of part A, and the porcentual error derived from these values.

Part A. Dimensions for part A can be seen in figure 25.

Figure 25: Part A dimensions

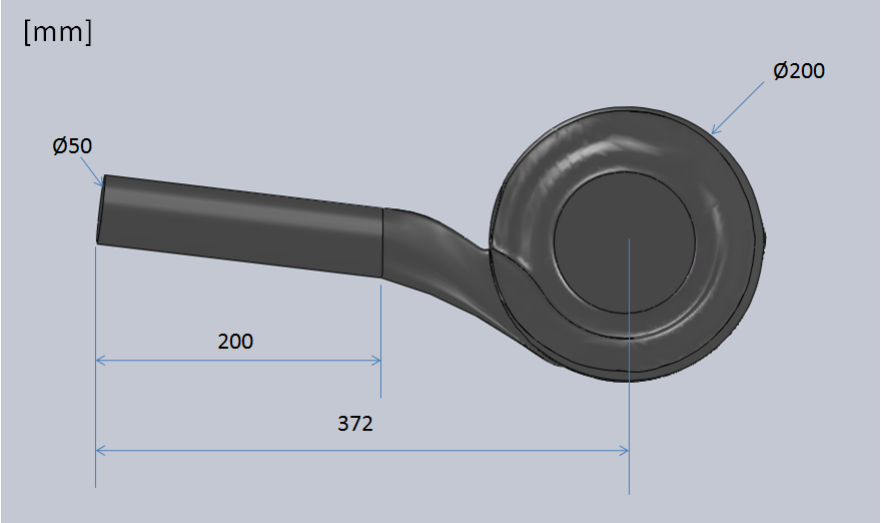

Table 2 offers a comparison between real and CAD dimensions for part A.

Table 2: Part A measurement comparison

Measurement	Real [mm]	Digitizing process [mm]	Error [%]
Volute inlet	49	50	2
Volute diameter	$\varnothing 205$	$\varnothing 200$	0.5
Volute center to inlet	175	172	0.6
Volute height	85	75	11.76
Volute outlet	$\varnothing 75$	$\varnothing 75$	0

It can be seen there are no great variation between real and digitized models. Volute height shows a error value of 11.76% justified by part manipulation by means of

boolean operations.

Part B. Only main diameters of part B are listed in figure 26 . It is important to mention that other degree thesis is dealing with a more detailed reverse engineering process for this part.

Figure 26: Part B dimensions

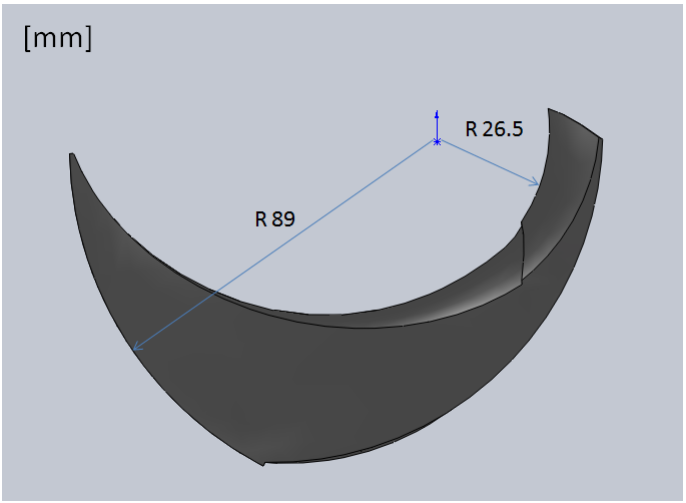

5.4 **Conclusions of the chapter**

The following are the conclusions for chapter 5

1. Two methods for digitizing of physical models were applied in a successful manner. (Laser scanner and arm-digitizing)

2. Scanning method presented advantages over point capture method, allowing the user to capture detailed geometry with high–resolution in less time.

3. Dimensions of digitized parts presented no considerable deviation from dimensions of real parts. It is important to clarify that due to the complexity of geometry a simplification of the computational model was made.

6 MESHING PROCESS

Inside general CFD process there is one requirement that must be performed before the simulation.

Meshing process is important because the CAD models must be tranformed in elements made out of geometrical primitives like hexahedra and tetrahedra in 3D, and quadrilaterals and triangles in 2D. Computational domains are split into smaller subdomains and discretized so governing equations are solved inside each of these portions of the domain (CFDOnline, 2009). The importance of meshing process relies upon the capacity to solve pertinent equations in the nodes of each element. The general process starts importing or creating geometry,rapairing geometry and then setting up global and local meshing parameters. The user selects the appropriate grid generation module to create the computational grid (ANSYS, 2009).

6.1 **Domain definition**

Definition of the domain is a must to do in order to achieve valid results without avoiding important features from the physical model. There is a need to define meshing domains for each of the digitized parts and then to assembly them inside CFX software. ICEM software presents diverse possibilities for structured and unstructured meshing, automatic or manual mesh creation. The strategy is to generate manual structured meshes, based on hexahedrical elements in order to have more accurate development of simulation and the possibility for refining special zones of the geometry (i.e impeller blades for boundary layer separation capture). An example of a hexahedrical element can be seen in figure 27.

Figure 27: Example of hexahedrical element

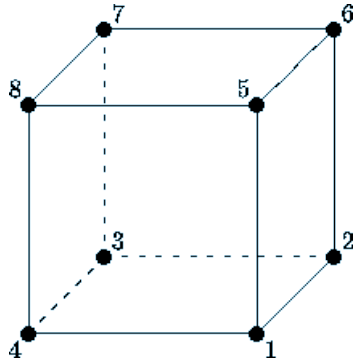

The computational domain is where the partial differential equations of the model will be solved. Simply stated as the division of the geometry in cells, made up from lines and nodes where solutions are developed. In the present project the domain will be subdivided for each digitized part and then assembled, having in mind the importance of good interaction between the meshes of each subdivision guaranteeing continuity. An example of 2D computational domain can be seen in figure 28

Figure 28: Example of Computational domain

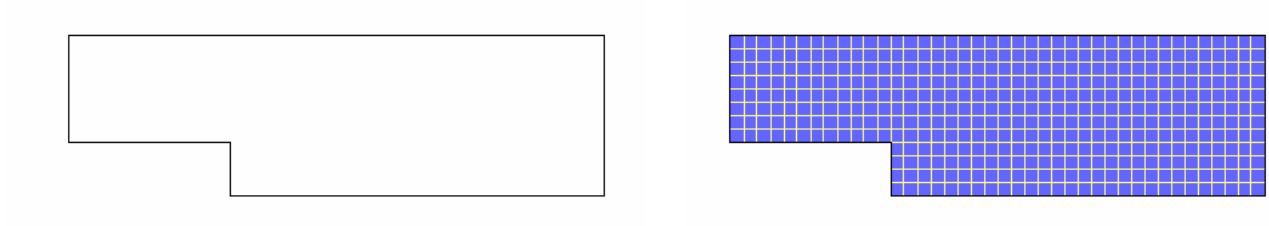

(a) Geometry

(b) Computational domain

(CFDOnline, 2009)

Subdivision of the domain is denoted with letters in order to avoid misunderstanding between names and regions from each one of the parts (see figure 29). This schema is the one used throughout the whole process and is the same as the one stated in

previous digitizing section

Domain A: Volute assembly

Domain B: Impeller duct

Domain C: Discharge pipe

Figure 29: Domain division

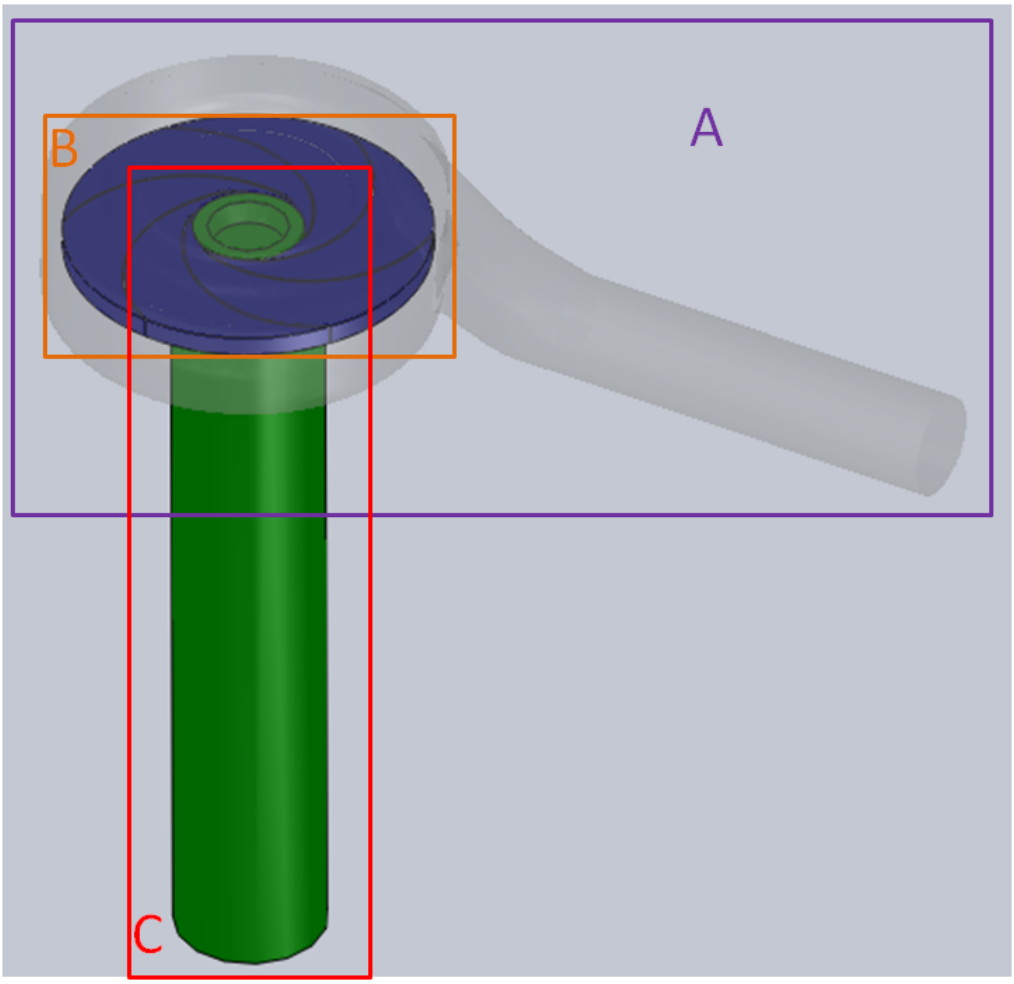

In the next section after presenting meshes for all the parts of the PAT, mesh information will be summarized in a table

6.1.1 **Domain A** The first model to define meshing domain is the volute assembly, denoted as A. Studying the part allows one can see that the inlet surface is clearly defined as well as the inlet pipe and volute geometry. Geometry is imported into the software in parasolid file format *.x_t*. This format takes all of the geometry from the original Solidworks file and permits good handling of geometrical features such as points, lines and surfaces. The consideration for the mesh inside the volute is that it does not require special attention excepting the place where the interaction with the impeller is going to be placed, because detailed definition of interfaces must be obtained and different regions of the domain can be discretized by less number of elements, in order to save computational time.According to complex geometry of the volute and the statement presented above, a tetrahedrical mesh is built, following parameters of maximum element size. A refinement was made in regions (A1) and the interface with the volute (A2).

Figure 30: Domain A regions

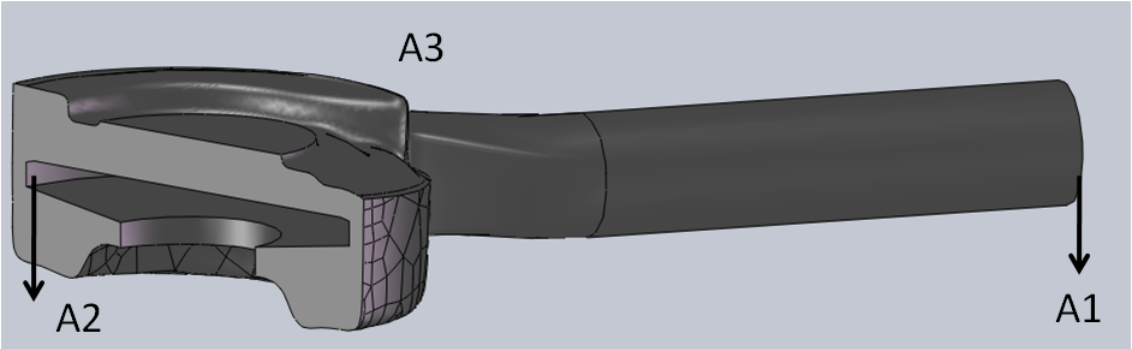

The tetrahedrical mesh for domain A can be seen in figure 31

Figure 31: Mesh for domain A (PAT Inlet and volute)

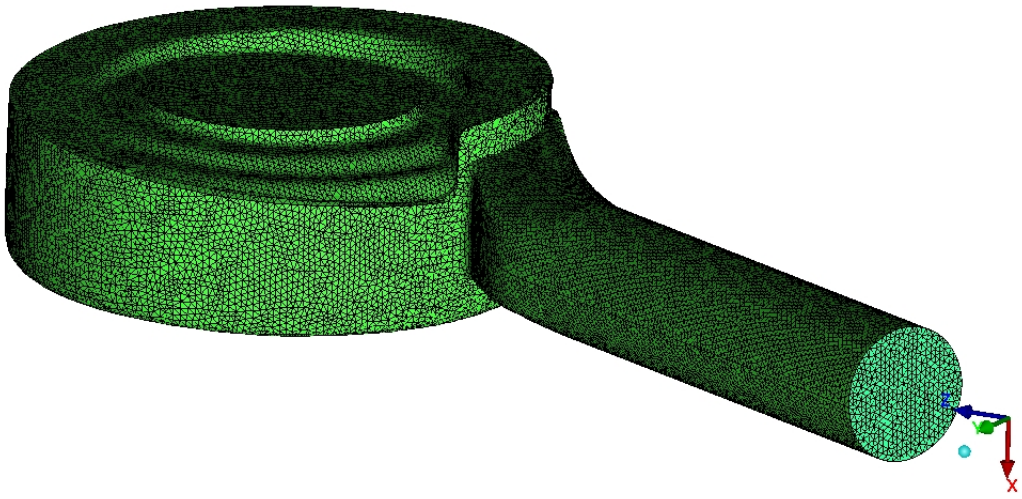

6.1.2 **Domain B** The meshing process for the impeller requires attention in some regions of the geometry. A hexahedrical mesh is created following parameters of grid spacing. The impeller geometry is divided in regions to make easy the selection of refinement geometry as seen in figure 32

Figure 32: Domain B regions

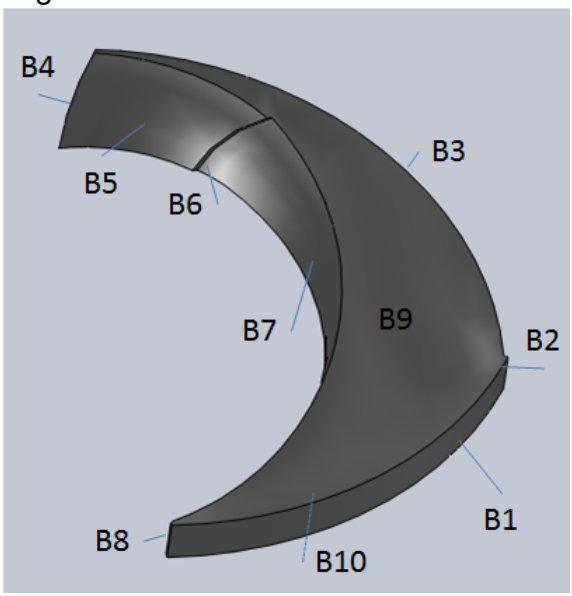

A block is created around the geometry for structured element creation and then divided into 11 blocks distributed through the fluid duct (see figure 33).

Figure 33: Blocking for domain B (PAT Impeller)

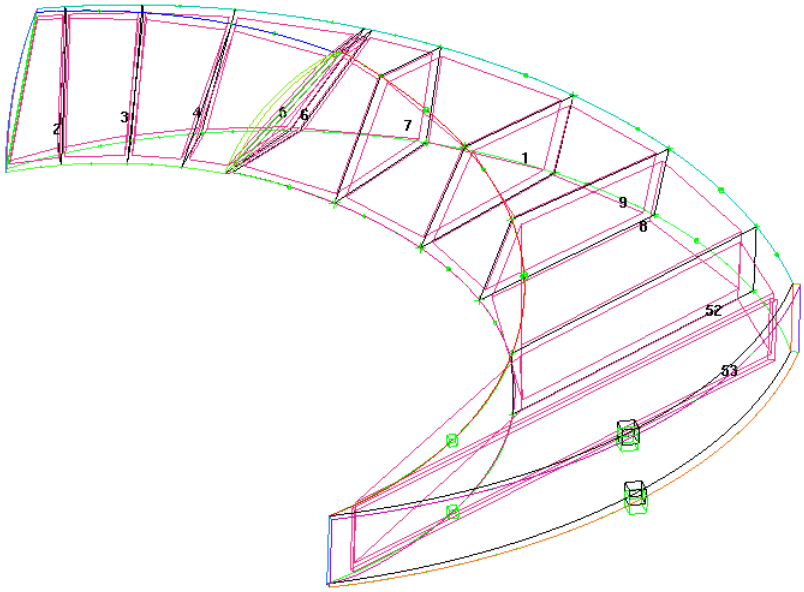

Edges and faces from the blocks are associated with curves and surfaces respectively. This association makes possible the correct adaptation to the geometry

When the association is complete spacing of edges is the step to follow. Edge parameters include spacing and geometrical distribution of nodes, which can be linear, spline, hyperbolical, etc. The preferred for this part is the default Bigeometrical option which gives good element spacing excepting regions in contact with vanes where a Biexponential distribution assures less grid spacing near vanes' surfaces. To control effects of turbulence near the wall of vanes an important parameter need to be taken into account, *y plus (y+)*, defined as the dimensionless distance between the wall and first node of the grid (CFDOnline, 2009). Good spacing beyond the refinement of the wall is also required to give stability to effects of flow. Software developer recommends, for SST model, to put at least 10 nodes into the boundary layer region

and, for lower Reynolds numbers (i.e a small pump) the entire boundary layer might only extend to around $y+ <= 300$ (ANSYS, 2009). In this case, a fine near wall spacing is required to ensure a sufficient number of nodes in the boundary layer. These parameters are important to have elements with good distribution throughout the domain. Example of the behavior of the boundary layer resolution can be seen in figure 34. This is why a biexponential distribution of the mesh is required near the vanes' walls.

Figure 34: Boundary layer resolution

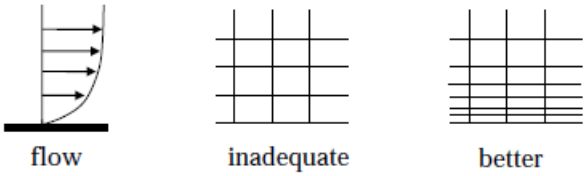

(BAKKER, 2002)

Computed mesh for part B evidences the distribution of elements near the wall of the vanes is seen in figure 35

Figure 35: Mesh for part B

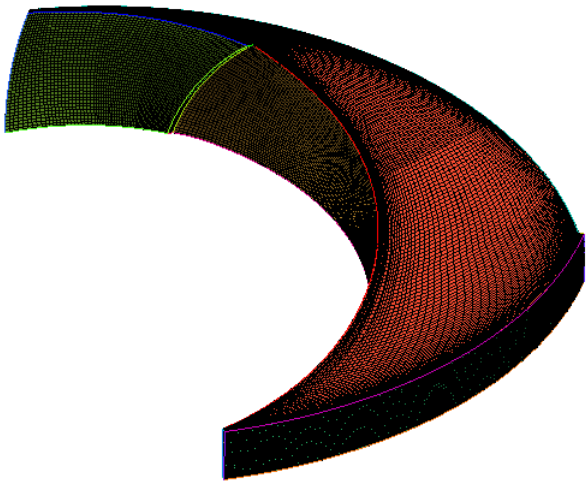

6.1.3 **Domain C** The shape of the PAT outlet is merely a pipe connected with the impeller following the geometry of the vanes. The advantage of this part is that the meshing process becomes a simple task, and the only place in focus being the interface between both impeller and pipe. The interaction should be guaranteed with the refinement of this region and the preservation of the O-grid feature, which is simply the modification of a single block or blocks to a 5 sub-block topology (7 sub-blocks in 3D) arranging grid lines into an “O” shape to reduce skew where a block corner lies on a continuous curve or surface(ANSYS, 2009). As described in 5.2.5 the lenght of the pipe is five times its diameter to observe a fully developed flow. As in the section 6.1.1,elements increment at C6 surface is required. As seen in figure 36 part C is divided in regions to define the interface with part B and definition of Boundary conditions.

Figure 36: Division for domain C (PAT Outlet)

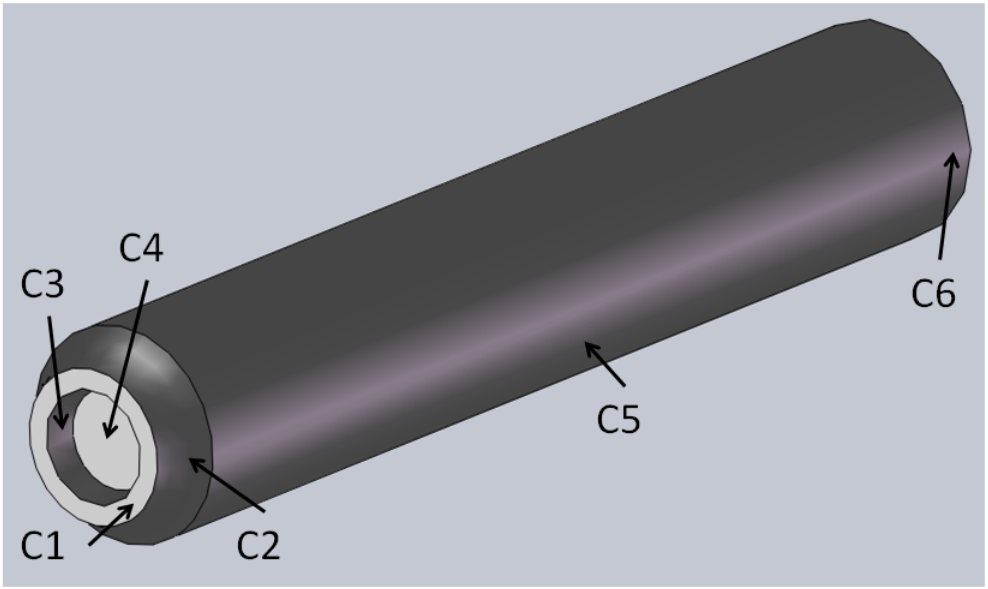

The blocking of domain C is done with the creation of 2 blocks and one o-grid block. Association of faces and edges is performed to assure correct adaptation of blocking features to the geometry.

Figure 37: Complete O-grid mesh for domain C (PAT Outlet)

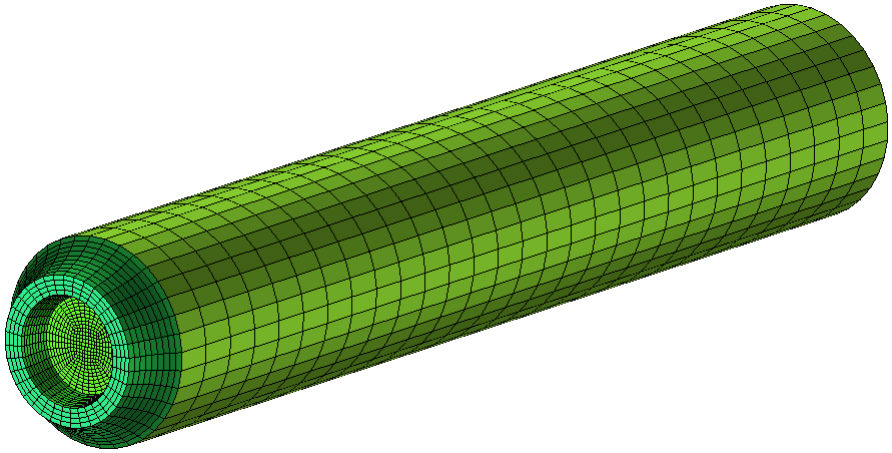

6.2 **Mesh quality check**

For the simulation, three meshes with different number of elements were created in order to perform analysis and study whether quality improvement affects the results and time of convergence by means of a mesh independence analysis.This procedure will be explained and applied to this project in next section. To coarsen or refine the existent mesh, modification of edge parameters and quality checks were the only tools used within software. These meshes are summarized in table 3

Table 3: Mesh quality

Mesh quality	Nodes	Elements
Low	372060	742687
Medium	1165537	1701845
High	1961171	2695180

It is essential to develop an analysis for the mesh quality, able to guarantee that the

amount of elements and nodes are independent from the solution.

6.2.1 **Mesh Independence analysis** Analysis of mesh independence consists in evaluating changes of a particular variable measured in the simulation with meshes of different quality. When the values for this specified variable remain unchangeable for several types of meshes, one can choose one of them whose amount of elements is adequate and permit good response in terms of convergence and computational time. For the present case, the analysis is done with calculation of torque along rotation axis, generated in all 6 vanes of the impeller and hub and shroud surfaces.Analysis values are listed on table 4 and figure 38.

Table 4: Mesh Independence analysis

Mesh Quality	Number of elements	Torque
High	2695180	1.441
Medium	1701845	1.439
Low	742687	1.425

The values for torque do not have a significant change in the medium and high quality meshes revealing that with medium quality meshes, good resolution can be obtained demanding less computational time.

Figure 38: Mesh Independence analysis

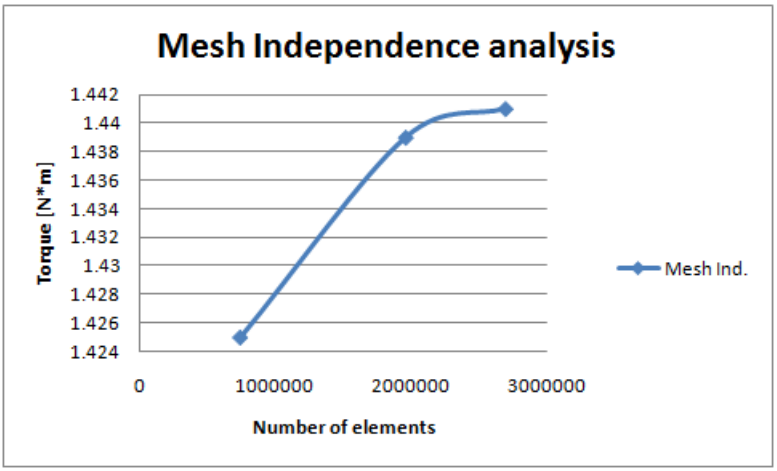

The values for *Y plus* were found to be less than the recommendation of the software developer and thus can give approximation to boundary layer management. The results for *Y plus* in relation with the mesh quality are seen in table 5

Table 5: Y plus and Mesh quality

Mesh Quality	Number of elements	Y plus
High	2695180	78.39
Medium	1701845	103.26
Low	742687	137.18

6.2.2 **Mesh quality check** Quality check is important to avoid trouble when simulating, especially to assure for example, wrong oriented elements or great skewness of elements. Some methods are used to evaluate mesh quality: determinant, orientation, aspect ratio, etc. For the present case, quality of all meshes are evaluated following determinant, max angle and aspect ratio. First, criteria for each one of

the chosen methods for quality inspection is explained and then a table will gather together the meshes for all the parts and values for quality.

Determinant criteria The criteria for evaluating determinant of jacobian matrix for the element is given by the software developer. A Determinant value of 1 would indicate a perfectly regular mesh element, 0 would indicate an element degenerate in one or more edges, and negative values would indicate inverted elements.(ANSYS, 2009)

Aspect ratio criteria An Aspect ratio of 1 is perfectly regular, and an Aspect ratio of 0 indicates that the element has zero volume.(ANSYS, 2009)

Maximum angle criteria Calculates the maximum internal angle of the quad or tri faces of elements. This value depends on the solver but it is recommended to have at least 9 or 18 degrees.(CFDOnline, 2009)

Each mesh was evaluated according these criteria and results are shown on table 6

Table 6: Mesh quality check

Quality criteria	Mesh A	Mesh B	Mesh C
Determinant	1.0	0.973	0.967
Aspect ratio	0.730	0.52	0.20
Max. Angle	140.6	119.88	109.89

These results show that good quality of meshes was obtained.

6.3 **Conclusions of the chapter**

The following are the conclusions for chapter 6

1. Combination of elements for dicretization of computational domains were created in order to permit the software to calculate accurately values.

2. Hexahedrical elements in the impeller are most suitable for obtaining more realistic results in turbulence modeling.

3. Because of geometrical complexity for structured meshing in the volute, a unstructured mesh made up from tetrahedrical elements was created. It showed good behavior in relation to grid association with structured mesh of the impeller allowing correct definition of interfaces, thus guaranteeing continuity inside the model.

4. Mesh independence analysis showed that decent results for the simulation can be achieved with low or medium quality meshes. This consideration reduces computational effort. Mesh quality check guaranteed that created domain meshes, are suitable for the simulation.

7 SIMULATION PROCESS

In the present project the goal is to approximate the conditions of a centrifugal pump during normal and reverse operation by developing numericals simulations and thus obtain the best operating conditions. Numerical model formulation will not be studied in dept because the complex behavior of turbulence. The implication of presenting turbulence in such terms will not obviate the basis for understanding the present problem or avoiding important items for setting up the chosen model. Simulation process deals with the correct imposition of boundary conditions to the meshes created previously. Physical variables for solving the numerical method inside the software must be defined following correct procedures in order to avoid senseless configurations. Parameters to achieve convergence of the model must be also defined.

The chosen model to perform the simulation is the shear stress transport model (SST) developed by Florian Menter on 1994 (MENTER et al., 2003). The selection of this model is based on its advantage to combine features from both k-epsilon and k-omega models to develop more realistic simulation of separation.(ANSYS, 2009) Regarding to PAT simulations, researchers like Rawal (see (RAWAL and KSHIRSAGAR, 2007)) had used the standard k-epsilon model because the case study was not fit to afford boundary layer influences and required effort only in obtaining reasonable solutions. Hence the use of k-epsilon model was only limited to find the values for dimensionless parameters regarding to flow rate, head and power. Authors like Sedlář in contrast, found to perform PAT analysis in terms of SST model evidencing large and small global separation (LGS, SGS) in impeller as well as reverse flow regions (RFR) inside impeller's passages. (see figure 39) (SEDLÁŘ et al., 2009)

Figure 39: Global separation in impeller (Turbine operation)

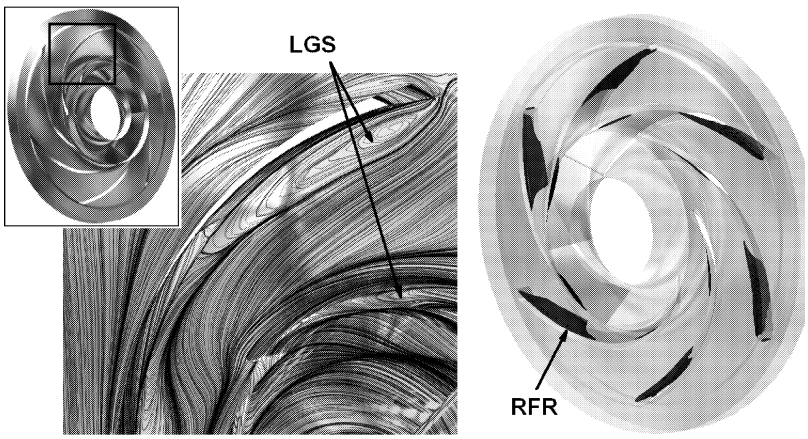

(SEDLÁŘ et al., 2009)

7.1 **Description of simulations**

The project will perform some simulations of the system in both operating modes. For the normal operation case, simulations in the BEP of the machine and values from the manufacturer provided curve will be carried out to verify and validate the behavior of boundary conditions and model.

On the contrary, in reverse operation the main interest is to evaluate several flow rate conditions at constant rotational speed, to find the BEP for the turbine operation and then, to make a comparison with predicted BEP from experimental methods developed by researchers worldwide. Simulations will be carried out to acquire in-

formation used as support for further experimentation. It is required to mention that the project will only provide data as reference for other researchers interested in the project focused specially in data acquisition and experimental measurements.

7.1.1 **Pump mode.** To begin the simulation process of the case study, simulation of the BEP for the system operating in pump mode is performed at a value for angular velocity of $1750[rpm]$. The main features of the pump to be used as well as its BEP (Operation conditions) are listed in table 7

Table 7: Goulds pump specifications

Technical Data:	GOULDS Centrifugal pump with metallic base and join guard
Model:	5SH 2 x 2 $\frac{1}{2}$ x 6
Operation conditions:	160 GPM@ 20 feet of water column
Engine:	TEFC 1.5 HP, 3ph. 220/440 Volts, 1750 RPM
Impeller:	Impeller for 5SH of 5 13/16” diameter

Other simulations at different points of operation are carried out to generate the characteristic curve of the pump numerically. These values were taken from the manufacturer characteristic curve in figure 7 and can be seen in table 8

Table 8: Pump values out of BEP

Q $[\frac{m^3}{s}]$	Q[gpm]	H[m]	H[ft]
0.0075	120	7.62	25
0.005	80	8.68	28.5
0.0025	40	9.60	31.5
0.0006	10	9.75	32

7.1.2 **Turbine mode.** For the case of the pump operating in turbine mode, the BEP will be achieved after simulation of several flow rates and then it will be compared to results calculated in an analytical manner. Before starting simulations of pump operating in turbine mode, BEP for turbine operation will be predicted by means of experimental equations developed by authors worldwide. Pump characteristic values at BEP are needed to find out appropriate BEP in turbine mode. These values were defined in table 7 Note that BEP will be achieved only for a defined value for rotational speed (N) of 1750 $[rpm]$.

The first method to concentrate in, is the one proposed by Sharma in (WILLIAMS, 2003). It is essential to determine pump specific speed to assure good prediction of BEP for turbine operation mode. According to (DERAKHSHAN and NOURBAKHSH, 2008) Sharma's methods are only accurate for pumps with specific speeds between 40 and 60 $\left(m, \frac{m^3}{s}\right)$

Specific speed can be calculated with equation 8

$$\begin{aligned} N_s &= \frac{1750[rpm] * 0.010[\frac{m^3}{s}]^{\frac{1}{2}}}{6.096[m]^{\frac{3}{4}}} \\ N_s &= 45 \end{aligned}$$

This value for specific speed allows one to perform BEP for PAT calculations following procedures of Williams manual.

Best efficiency conditions for pumps and turbines are different, though, PAT at BEP will be approximately the same as for pump operation. When operating as turbine, the head and flow required are greater than theoretical values thus making up for losses. In a centrifugal pump, energy losses cause the reduction of head and flow

from theoretical maximum values.

$$Q_t = \frac{Q_{bep}}{\eta_{max}} \tag{24}$$

$$H_t = \frac{H_{bep}}{\eta_{max}} \tag{25}$$

$$\eta_t = \eta_{max} \tag{26}$$

Experimentation has discovered that head ratio H_t/H_{bep} is usually greater than flow ratio . Improvement of calculation was proposed by KR Sharma of Kirloskar Co., India when turbine and pump speeds are the same:

$$Q_t = \frac{Q_{bep}}{{\eta_{max}}^{0.8}} \tag{27}$$

$$H_t = \frac{H_{bep}}{{\eta_{max}}^{1.2}} \tag{28}$$

Affinity laws are required to establish relationships between pump and turbine's speed. Running conditions at BEP can be calculated in the following manner:

$$Q_t|_{N=N_t} = \frac{N_t}{N_p} \cdot Q_t|_{N=N_p} \tag{29}$$

$$H_t|_{N=N_t} = \left(\frac{N_t}{N_p}\right)^2 \cdot H_t|_{N=N_p} \tag{30}$$

Now substituting these equations into equation 28

$$Q_t = \frac{N_t}{N_p} \cdot \frac{Q_{bep}}{\eta_{max}{}^{0.8}} \quad (31)$$

$$H_t = \left(\frac{N_t}{N_p}\right)^2 \cdot \frac{H_{bep}}{\eta_{max}{}^{1.2}} \quad (32)$$

As stated by Williams, this method results more accurate than equations stated in equation 26, however it is still an approximation (WILLIAMS, 2003). Values for Q_t and H_t may be as much as $\pm 20\%$ of the predicted value for BEP, having , significant effects or not on PAT output, depending the case and performance characteristics. It is recommended to test the pump as a turbine, finding out power produced at available head and flow.

For the present case assumption of the same rotational speed is stated, therefore calculations can be performed using equations 28

Prediction of flow rate in turbine operation

$$Q_t = \frac{0.010}{0.66^{0.8}}$$

$$Q_t = 0.0139[\frac{m^3}{s}]$$

Prediction of head in turbine operation

$$H_t = \frac{6.096}{0.66^{1.2}}$$

$$H_t = 10.037[m]$$

In the same way another approach for flow rate is going to be calculated with the procedure developed by (DERAKHSHAN and NOURBAKHSH, 2008) consisting in

the use of non-dimensional head, flow and power coefficients in relation to pump and turbine rotational speed, flow and head at pump BEP and pump's power input.
This method was set up after collection of experimental data and as declared by the authors it is valid only if it accurately predicts both head ratio and flow rate ratio simultaneously for a given range of specific speeds and since the method was based only on four experimental data, it may not be accurate for all centrifugal pumps becoming a task to be, the acquisition of more experimental data in order to improve its accuracy. In the beginning, the method presents three main equations in which values for flow rate, head and turbine power need to be calculated after pointing out pump and turbine dimensionless parameters. Subscripts are defined to be *t* for turbine and *p* for pump

$$\varsigma = 0.0233\alpha_p + 0.6464 \tag{33}$$

$$\alpha_t = 0.9413\alpha_p – 0.6045 \tag{34}$$

$$\beta_t = 0.849\beta_p – 1.2376 \tag{35}$$

Pump and turbine dimensionless specific speeds are calculated with the following relations and replaced altogether with dimensionless parameters in equations 33, 34 and 35

$$\alpha_p = \frac{N_p Q_p^{0.5}}{(g * H_p)^{0.75}} \tag{36}$$

$$\beta_t = \frac{N_t P_t^{0.5}}{\rho^{0.5} (g * H_t)^{1.25}} \tag{37}$$

α_p $[m, \frac{m^3}{s}]$ and β_t [m, W] are the dimensionless specific speeds. In a similar manner, these are the required parameters.

$$\varsigma = \frac{N_t}{N_p}\left(\frac{H_t}{H_p}\right)^{-0.5} \tag{38}$$

$$\alpha_t = \frac{N_t Q_t^{0.5}}{(g * H_t)^{0.75}} \tag{39}$$

$$\beta_p = \frac{N_p P_p^{0.5}}{\rho^{0.5}(g * H_p)^{1.25}} \tag{40}$$

Substituting all relevant relations into three main equations for predicted flow, head and power, a system of equations is achieved and solved for H_t and Q_t which are the desired BEP prediction values for setting up the simulations. The rotational speed of the turbine is assumed to be $1700[rpm]$

$$\frac{N_t}{N_p}\left(\frac{H_t}{H_p}\right)^{-0.5} = 0.0233\frac{N_p Q_p^{0.5}}{(g * H_p)^{0.75}} + 0.6464 \tag{41}$$

$$\frac{N_t Q_t^{0.5}}{(g * H_t)^{0.75}} = 0.9413\frac{N_p Q_p^{0.5}}{(g * H_p)^{0.75}} - 0.6045 \tag{42}$$

$$\frac{N_t P_t^{0.5}}{\rho^{0.5}(g * H_t)^{1.25}} = 0.849\frac{N_p P_p^{0.5}}{\rho^{0.5}(g * H_p)^{1.25}} - 1.2376 \tag{43}$$

To calculate turbine hydraulic power, pump input power P_p is taken from equation 12 and its relationship with motor efficiency and electrical power

$$P_{elec} = 1.5[HP] = 1185[W]$$

$$P_p = 1185\frac{66}{100}P_p = 782.1[W]$$

The reached value for Turbine hydraulic power at BEP (P_t) should be used to be compared with results from the simulation

After solving the system of equations predicted values are found to be

$$\begin{aligned} H_t &= 8.23[m] \\ Q_t &= 0.008[\frac{m^3}{s}] \\ P_t &= 879.92[W] \end{aligned}$$

Other ways to predict BEP were developed by other authors and explained in the following paragraphs according to documentation compiled by (ORTIZ and ABELLA, 2008). Because there are not enough information about pumps operating in turbine mode, experimental methods had been developed to point out the BEP of the machine; these methods are based on hydraulic characteristics from pump mode. To generalize the way the calculations are carried out, predicted flow, head and efficiency have a relationship with coefficients denoted as (K). Remember that *t* and *p* are the subscripts for turbine and pump respectively.

$$Q_t = K_Q Q_p \tag{44}$$

$$H_t = K_H H_p \tag{45}$$

$$\eta_t = K_\eta \eta_p \tag{46}$$

These coefficients establish a relationship for BEP values for both modes of operation. In table 9, values for these coefficients are presented in terms of pump's efficiency.

Table 9: Flow, head and efficiency coefficients in relation with pump efficiency

Ref.	K_Q	K_H	K_η
Stefanoff	$\frac{1}{\eta_p^{0.5}}$	$\frac{1}{\eta_p}$	1
Mc. Claskey	$\frac{1}{\eta_p}$	$\frac{1}{\eta_p}$	1
BUTU	$\frac{0.85\eta_p^5+0.385}{2\eta_p^{9.5}+0.205}$	$\frac{1}{0.85\eta_p+0.385}$	$1-\frac{0.03}{\eta_p}$
Krivchenko	$0.9-1.0$	$1.56-1.78$	$0.75-0.8$

After solving each one of the expressions in the table, these are the predicted values for PAT's BEP.

Table 10: Predicted Flow, head and efficiency values for turbine operation

Ref	$Q_t[\frac{m^3}{s}]$	$H_t[m]$	$\eta_t[\%]$
Stefanoff	0.0123	9.2364	0.66
Mc. Claskey	0.0152	9.2364	0.66
BUTU	0.0202	12.404	0.63
Krivchenko	0.010	10.363	0.53
Sharma	0.0139	10.037	0.66
Derakhshan	0.0075	8.23	0.66

Calculated values are then compared with simulation results to see which method approaches a better solution and then compared with the desired value for energy generation. Mechanical power is the amount of energy the impeller will be receiving due to the energy transformation between the fluid and the vanes to generate rotational movement. This mechanical energy is the usable energy that can be taken from hydraulic power in the fluid at the impeller.

This energy is the one to be converted into electrical energy by the operation of the

motor as generator. It is important to mention that electrical considerations are out of the scope of this project. The obtention of mechanical power in the shaft is the purpose of the project.

Mechanical power can be obtained from calculation in the post–processing tool, using special notation for finding out the torque in energy generation axis of the impeller and multiplying it with the angular velocity of the impeller according to the well known equation in 48. The value for torque is reached by integration of this variable in the hub, shroud and six vanes' surfaces of the impeller. Variable to be used inside the software is $"torque\_x"$.

$$Impellertorque\,(\tau) = torque\_x()@blades + torque\_x()@wall\_b \tag{47}$$

τ=Impeller Torque $[Nm]$

$torque_x()$=Software variable calculated in generation axis

@=Reference of surfaces where the variable is calculated

blades= Vanes' surfaces $wall_b$ = Hub and shroud surfaces

$$P_m = \tau\omega \tag{48}$$

P_m=Mechanical power [W]

τ=Impeller Torque $[Nm]$

ω=Angular velocity of the impeller [rps]

This value for mechanical power should not exceed the value for the electrical power of the motor ($1185[W] = 1.5[HP]$) in order to avoid overheat in the operation of the motor and possible damage. A schema showing how the energy is transformed in

the domain can be seen in figure 40. The hydraulic power available in the fluid is transformed into mechanical power in the shaft by means of rotation movement of the impeller and close relationship with pump efficiency.

Figure 40: Energy transformation in the system

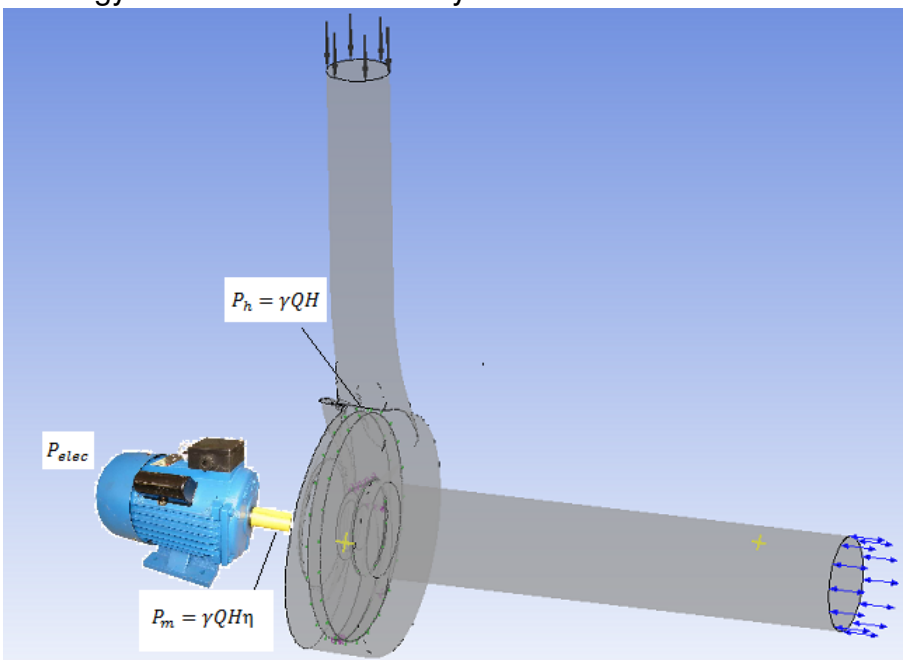

7.2 **Boundary conditions**

Treatment of the model requires the definition of boundary conditions through all the domain, becoming a key feature for the success of the simulation.

- BC are required for the mathematical model
- Boundaries direct motion of flow
- BC specify mass, momentum and energy fluxes into the computational domain
- Incorrect boundary conditions will lead to incorrect results

- Wide range of boundary conditions permit flow to enter and exit solution domain (BAKKER, 2002)

Short description of commonly used boundary conditions for hydromachinery is summarized and then extended to the present problem. Definition of fundamental boundary conditions will lead to correct set up of the PAT simulation inside CFX.

Table 11: Common Boundary conditions

Boundary name	Description
Inlet	Permit the flow to enter the solution domain
Outlet	Permit the flow to leave the solution domain
Wall	Permit to distinguish fluid and solid regions
Symmetry	Permit the reduction of computational effort in problem
Periodicity	Permit the reproduction of a periodically repeating nature

This section involves the whole definition of the boundary conditions for the different subdomains in each one of the parts of the pump in normal and reverse operation. After defining each part, full model conditions will be exposed. According to the defined subdomains in meshing section, boundary conditions will follow the letter notation for better understanding.

7.2.1 **Pump mode BC** First consideration for the simulation is to perform pump conditions. Ansys recommends that best results can be achieved by defining a total pressure condition at inlet and mass flow rate at outlet of the control volume. Flow rate at BEP as well as for values from pump manufacturer chart are going to be used at pump outlet. CFX input conditions are now specified.

Analysis type The system is analyzed in steady state, meaning that variables of interest for the simulation such as velocity and turbulence parameters are going to remain constant in time.

Material type The fluid is water at 25 [C] as a standard suitable value for pump conditions in the region. There is no need to define specific parameters regarding to fluid (viscosity, density, etc) because CFX assumes its established values for these material properties.

Domain definition In both states of the pump, three domains are defined according to each one of the parts of the system. Definition of the domain is important because here is where equations are solved. Required parameters are the following:

- Reference pressure: In order to keep coherence between total pressure of system and slight changes in dynamic pressure, the value for this variable is set as 1 [atm] and must be used for all other domains involved in the simulation (ANSYS, 2009). In other words it is the datum from which all pressure measurements are specified.
- Buoyancy: No buoyancy is chosen because there are neither gravitational nor density changes in the domain
- Domain motion: This option allows the user to define whether the domain is stationary (fixed) or if it is rotating. For sections A and C (part A and C) there is no domain motion so they are defined as stationary while section B must be a rotating domain at constant angular velocity of 1750 [rpm]

- Heat transfer model: Heat transfer is not involved in the process because heat flow is not of interest as so fluid through vanes, therefore Isothermal model at 25 $[^{\circ}C]$ is set up
- Turbulence model: As stated at the beginning of the chapter the model to be used is Shear Stress Transport because of its strong behavior in simulating turbulence and near wall effects.

Now particular boundary conditions for each section of the geometry will be defined.

Domain A Several values for flow rate in pump mode according to provided pump curve are tested and summarized. In section A the outlet of the pump operating in pump mode is located and parameters imposed.

- The circular surface denoted as A1 is the outlet surface where a condition of mass flow rate is specified. For each one of the flow rates from the curve (160,120,80,40,10 gpm), mass flow values were calculated.

Table 12: Inlet mass flow rate values

Sim.	$\dot{m}[\frac{kg}{s}]$
1	10
2	7.5
3	5
4	2.5
5	0.6

- There is an interface condition for the surface of section A in contact with the impeller, denoted as A2,where conservative flux for mass and momentum's conservation equations, is chosen to preserve consistency of models through the interface.

- The condition for the solid part (A3) is defined as *No slip wall* with smooth surfaces. This condition assumes that tangential velocity of the fluid immediately next to the wall is equal the velocity of the wall.

Domain B Boundary conditions for section B are basically wall and interface conditions

- Region B1 of the impeller channel is where the fluid is going to leave domain B and enter the volute. As described in meshing section, refinement of this zone was required. This region connects the volute with an interface condition preservating continuity.
- Regions B2,B4,B6 and B8 require a periodicity condition regarding to rotation axis.
- Vanes will have a condition of No slip wall.
- Region B5 is where the fluid coming from part C enters B domain. This interaction involves the rotational movement of the impeller, leading the implementation of a rotational interface. Frozen rotor model is required for correct adaptation of meshes between domains. This model employs a quasi-steady algorithm where the rotor and stator are modeled at a fixed (frozen) position relative to each other. The two frames of reference connect in such a way that they each have a fixed relative position throughout the calculation.

  Recommendations of the Frozen Rotor model are given by the software developer (Ansys) arguing it must be used for non-axisymmetric flow domains, such as impeller/volute, turbine/draft tube, propeller/ship and scroll/volute cases. It can also be used for axial compressors and turbines. The Frozen Rotor

model has the advantages of being robust, using less computer resources than the other frame change models, and being well suited for high blade counts.(ANSYS, 2009) As stated in section 7.1 simulations are first run with Frozen rotor model and then results are input to a new simulation with Stage model. This model instead of assuming a fixed relative position of the components, performs a circumferential averaging of the fluxes on the interface so solutions are then obtained in each reference frame. The Stage model usually requires more computational effort than the Frozen Rotor model to converge. This model is most applicable to axial machines, compressors and pumps with return or outlet diffusers.(ANSYS, 2009)

Domain C Boundary conditions in section C are meant to define completely the simulation for the pump operating in pump mode.

- The inlet condition is applied where the flow is entering the domain, this is the circular face at the pipe in section C (C6). The flow condition at this point is subsonic regime because velocity is below sound velocity. Mass and momentum condition is static pressure of 9810 [Pa] assuming as if the pump were submerged one meter in deposit. Turbulence condition and flow direction are taken as Zero gradient which implies that turbulent conditions are fully developed in the suction from the tank.
- No slip wall condition is applied in regions C1,C3,C4 and C5.
- The same interface condition stated for section B is required for section C in order to preserve continuity in the solution of equations.

Figure 41: Boundary conditions for pump operation

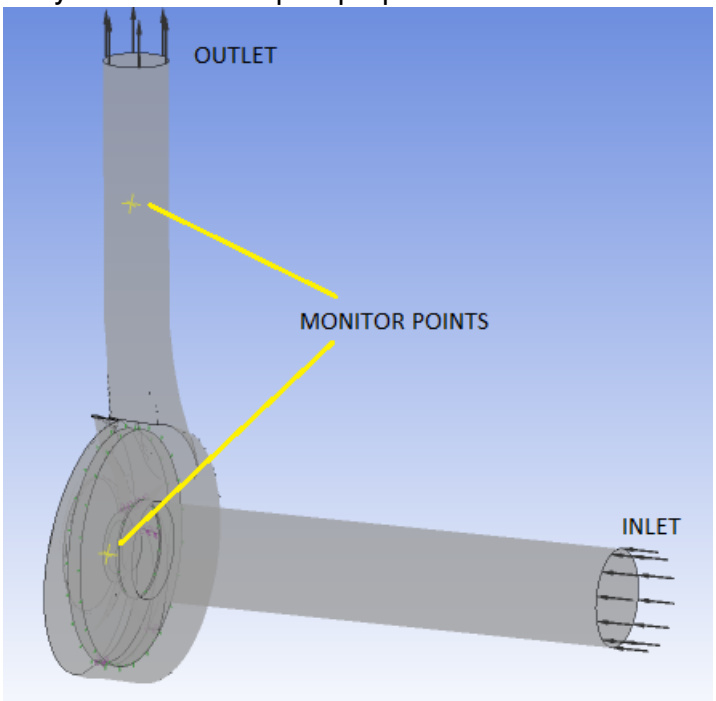

7.2.2 **Pump as Turbine BC** Boundary conditions for the pump operating in turbine mode are selected after predicting the values for BEP. The presented model configuration is the same for all the input values from each one of the experimental models.

Analysis type As in the pump simulation, the system is analyzed in steady state.

Material type Fluid condition is the same, water at 25 $[°C]$

Domain definition Definition of the domain for turbine operation requires minimal changes in key features from boundary conditions.

- Reference pressure: Remains the same as for pump mode.

- Buoyancy: No buoyancy is chosen because there are neither gravitational nor density changes in the domain.
- Domain motion:For sections A and C (part A and C) there is no domain motion as in pump mode, while in section B,the angular velocity for the domain must be changed to -1750 [rpm], because the reversed direction of flow.
- Heat transfer model: In the same manner for pump mode, heat transfer is not considered
- Turbulence model: As stated before, the model to be used is Shear Stress Transport.

Because of fewer changes in turbine mode,particular boundary conditions for each section of the geometry must be considered and re–defined.

Domain A Boundary conditions for this domain are defined in terms of flow rate as in pump mode, but differ in the boundary conditions that will be used.

- The circular surface denoted as A1 becomes now to be the inlet surface. A condition of mass flow rate is specified in this section. Each one of the predicted flow rates according to mentioned authors, are the inlet condition for each simulation. Input values are taken from table 10. Turbulence parameters are, turbulence kinetic energy (k) and turbulent dissipation energy (ε). Turbulent kinetic energy is associated with eddies in turbulent flow, it can be calculated with this expression.

$$k = \frac{3}{2}U^2 I^2 \tag{49}$$

k=Turbulent kinetic energy

U=Velocity magnitude

I=Turbulent intensity

Turbulent dissipation energy (ε) is the rate at which the velocity fluctuations dissipate in turbulent flow, it can be calculated with this expression

$$\varepsilon = \frac{k^{\frac{3}{2}}}{0.3D_h} \tag{50}$$

ε=Turbulent dissipation energy

k=Turbulent kinetic energy

D_h=Hydraulic diameter at inlet

According to Ansys in CFX's reference manual, when there exists no idea about turbulence levels, it is recommended a value of 5% for turbulence intensity. For this case Turbulence intensity will be defined to be high (10%), because of complex geometry inside the volute and suppositions of turbulent flow in the system.

- The interface condition for the surface of section A in contact with the impeller (A2) remains the same as for pump mode.
- The condition for the solid part (A3) is defined as *No slip wall* with smooth surfaces.

Domain B Boundary conditions for section B are basically the same conditions used for pump mode simulation (see section 7.2.1) The only difference is the direction of the flow crossing the impeller. B1 region now will be the zone where the fluid is entering the domain and B5 where it is leaving the domain.

Domain C Boundary conditions for domain C can be seen in figure 42 and are described as follows

- In a different way regarding pump mode, the outlet condition is applied at the circular face at the pipe in section C (C6). The flow condition at this point is static pressure at 1 [atm] because the fluid is leaving the outlet pipe.
- No slip wall condition is applied in regions C1,C3,C4 and C5.
- The same interface condition stated for section B is required for section C in order to preserve continuity in the solution of equations.

Figure 42: Boundary conditions for Turbine operation

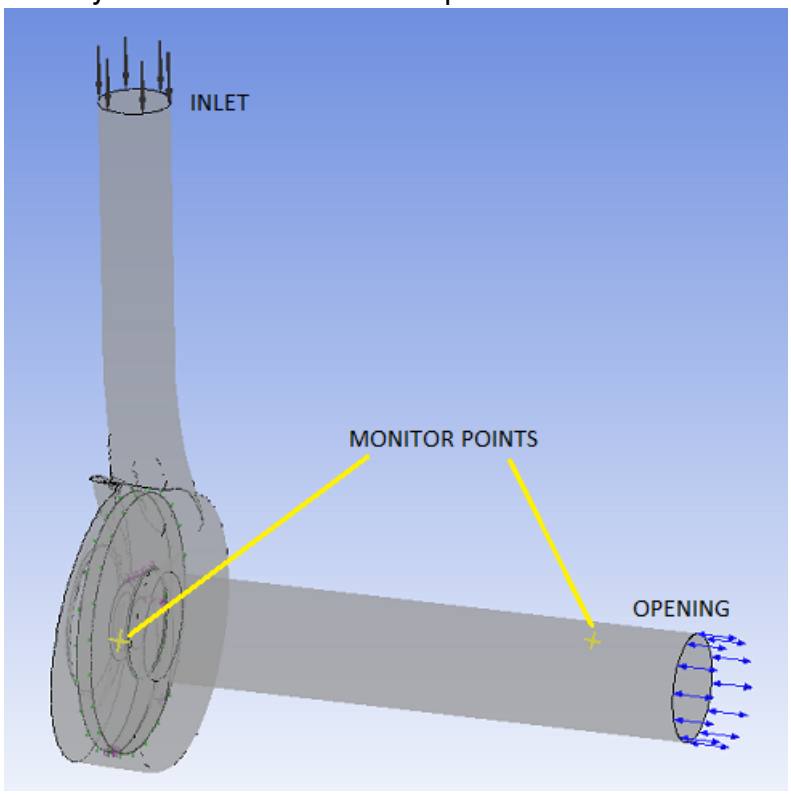

7.3 **Solver parameters**

Parameters for setting up model's convergence are important because an accurate solution depends on these values. To control the way the equations for imposed parameters that have to be solved in each one of the domains, few items inside the solver control must be defined.

- Solution units: Solution units are based on the metric system $[kg, m, s, ^\circ K, rad]$.
- Convergence control: Total number of iterations are determined according behavior of the simulation. For all simulations this number did not exceed 150. Most engineering applications require between 50 to 100 iterations to converge(ANSYS, 2009). Maximum limit of iterations should not exceed 200.
- Convergence criteria: Regarding to convergence parameters it is required to consider the size of the RMS residual, the size of the MAX residual, as well as the overall flow balances (overall conservation).(ANSYS, 2009) The RMS residual level applied in all simulations was 1e-05 according Ansys advice: "1e-5 is good convergence, and usually sufficient for most engineering applications."(ANSYS, 2009)
- Advection scheme: A high-resolution scheme is used to calculate flow equations in regions where gradients vary considerably (ANSYS, 2009)
- Timescale control: Automatic timescale control and conservative lenght scale factor are used to achieve a solution in reasonable time due to chraracteristics for this configuration as stated by Ansys, ...for steady-state problems, the CFX-Solver applies a false timestep as a means of under-relaxing the equations as they iterate towards the final solution(ANSYS, 2009)

Convergence for the simulations is shown in figure 43

Figure 43: Residuals for Turbine operation

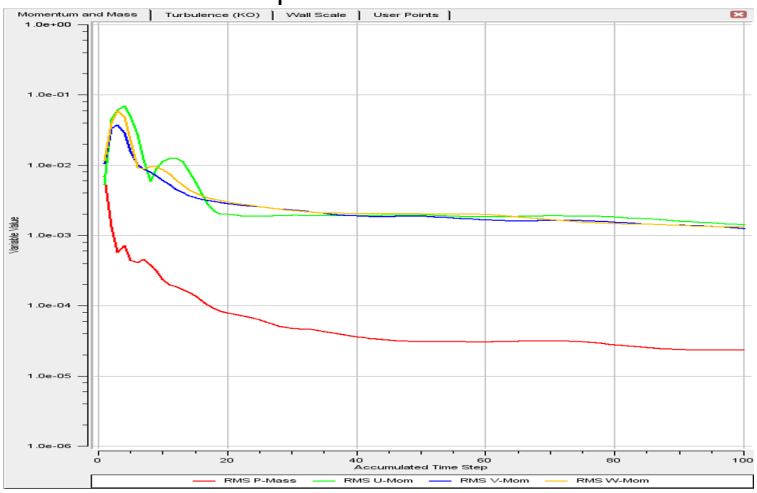

7.4 **Output control**

This section provides the option for the user to perform monitoring variables anywhere inside the simulation. In the present case, two monitoring points were located at volute and outlet for both modes of operation. The duty of these points was to help the monitoring of the simulation and see whether convergence was being achieved. The variables for both points were absolute pressure.

Monitor points are shown in figure 44

Figure 44: Monitor points for Turbine operation

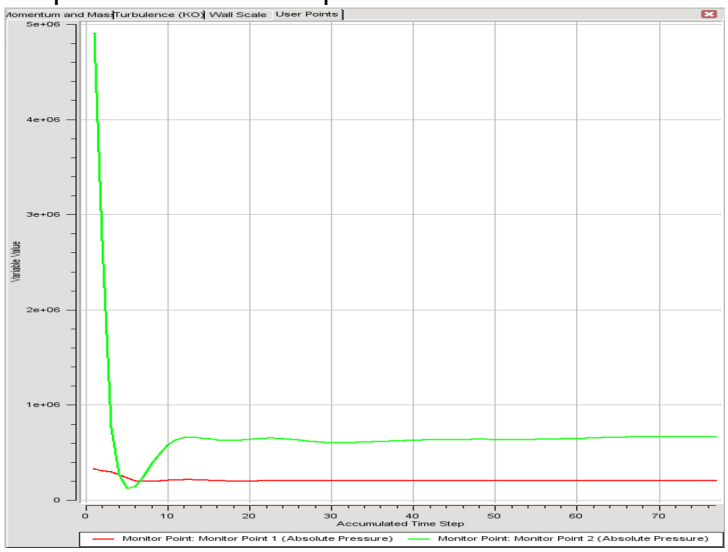

As the values for the pressure at monitor points stabilize , convergence is achieved.

7.5 **Conclusions of the chapter**

The following are the conclusions for chapter 7

1. The boundary conditions that were implemented in the model, showed good convergence and presented results in a reasonable time.

2. With experimental prediction of BEP some data is found for making a comparison with simulation results.

3. Both conditions of operation for the pump were simulated without encountering problems.

8 RESULTS AND DISCUSSION

This chapter deals with the results for the simulation of the pump operating in both modes. First, a description of procedure and results for the pump operating in its original scenary is exposed. After collecting all the information about pump results, simulation results for the pump in turbine mode are described and analyzed. It is valid to remember that two types of simulations were carried out. First type was the simulation of the pump operating in pump mode at values taken out from the pump's manufacturer curve. The idea with this procedure was to make an approach of pump conditions. The second type of simulation considered the reverse operation of the pump at several conditions of flow rate in order to find the mechanical power able to be produced by the shaft. Both simulations were carried out at a fixed rotational speed of $1750[rpm]$.

8.1 **Pump mode results**

Pump mode simulations as said before in chapter 7 were carried out with different conditions regarding to flow rate. The idea is to plot the pump characteristic curve for each flow condition by finding values for head and comparing these curves with the one provided by pump manufacturer.

Total Head for each simulation was calculated according to Bernoulli's equation (equation 1) between suction side and discharge side of the pump, by means of integrated functions of the software. Post–processing tool offers the possibility to calculate Total pressure in any transversal section of the domain by mass flow functions. The function that permit one to find the value for the total pressure is called

massFlowAveAbs. This function takes the value for the pressure in any 2D region of the domain and weights it by mass flow. In a certain way it can be though to be the specific energy of the chosen transversal area.

In this manner, the expression $massFlowAveAbs(TotalPressure)@outlet$ calculates the average Total pressure on the discharge, weighted by the mass flow at each point on the location As total pressure is taken into account for the calculation,static,dynamic and elevation terms from Bernoulli's equation at each location (suction, discharge) are calculated performing a simple energy balance as follows.

$$H = \frac{P_d - P_s}{\gamma} \tag{51}$$

P_d=Discharge total pressure [Pa]

P_s= Suction total pressure [Pa]

γ=specific weight

The values for flow rate and head for each one of flow rate conditions in pump mode can be seen in table 13

Table 13: Flow and head for pump operation

Q $\left[\frac{m^3}{s}\right]$	H$[m]$	H$[m]$ (manufacturer)	Error(%)
0.010	7.63	6.096	20.1
0.0075	10.59	7.620	28.05
0.005	11.85	8.680	26.75
0.0025	11.77	9.600	18.44
0.0006	12.61	9.753	22.66

The resulting curve is plotted in figure 45 and compared with manufacturer's curve.

Figure 45: Pump operation curve

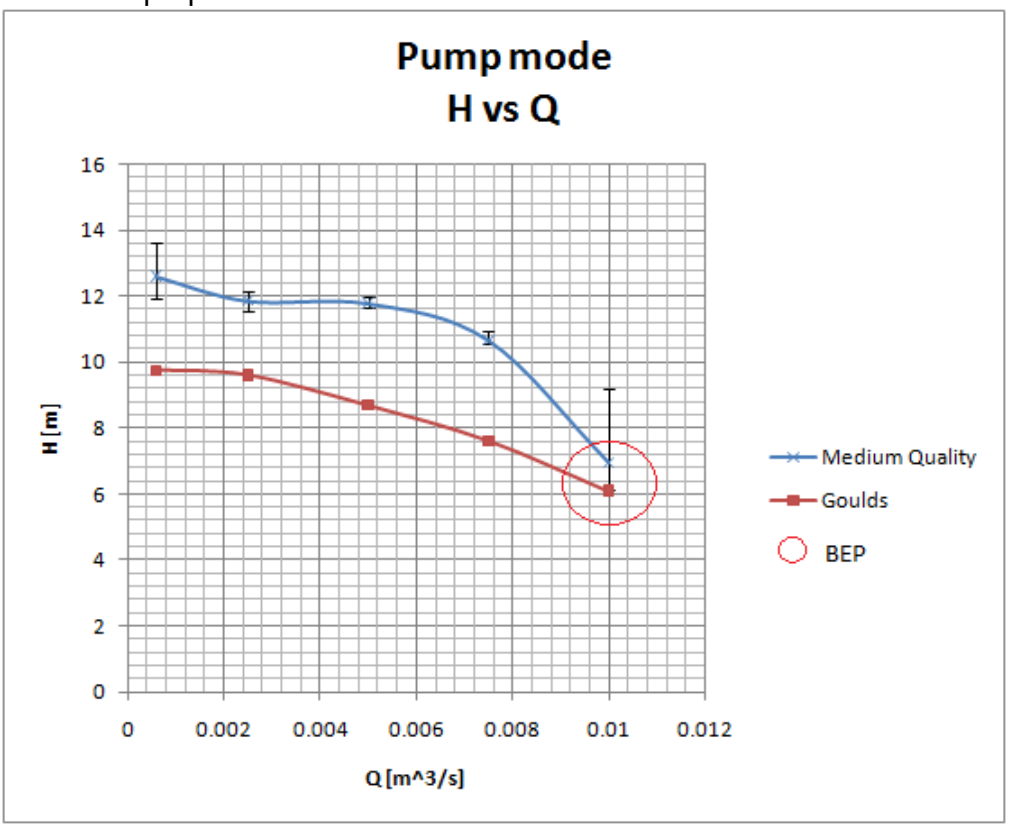

It can be seen the shape of the curve is similar to the one provided by Goulds. The curve of the pump was plotted with medium resolution of the mesh and reliability intervals show the variation with high and low quality meshes, above and below respectively. Simulated curve is over manufacturer's curve because inside the simulation neither losses nor other components such as seals, bearings, etc. were considered. In other words the efficiency of simulations was greater because losses were neglected.

The behavior of velocity vectors show that the fluid decelerates as it crosses through the impeller's ducts from the suction eye to the volute, revealing the typical behavior of the pump by means of increment of pressure. This behavior can be seen in figure

46. Rotation for pump mode is oriented according right hand measure to be along positive value for X axis.

Figure 46: Velocity vector and pressure field plot

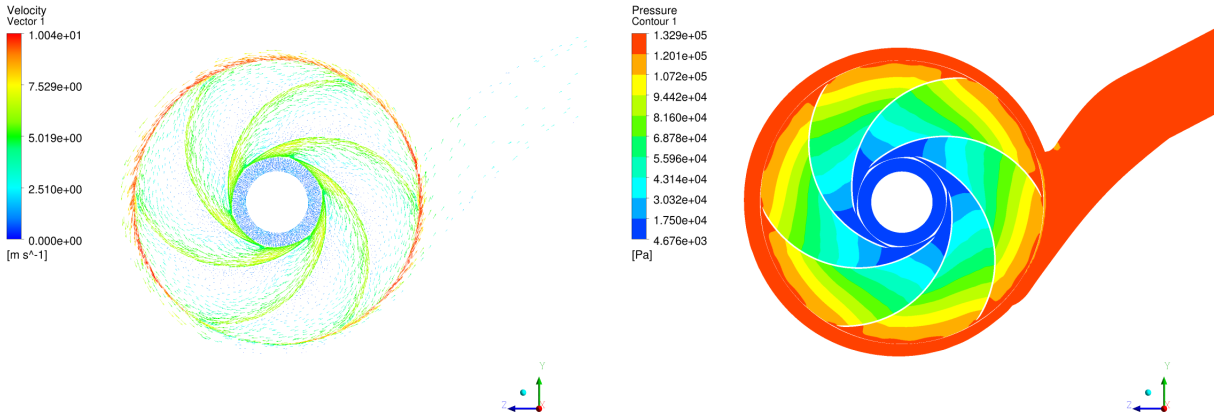

(a) Vector field pump mode

(b) Pressure field pump mode

8.2 **Turbine mode results**

After simulating the behavior of the pump operating in turbine mode at different flow rate conditions, values for total head were calculated in the same manner as the pump operation case. (See equation 51) These values are listed in table 14

Table 14: Flow and head for turbine operation

Q $\left[\frac{m^3}{s}\right]$	H$[m]$
0.010	15.01
0.011	17.34
0.012	20.29
0.014	26.44
0.015	29.7
0.020	51.26

Because efficiency is an important parameter to have a notion about turbine performance, efficiency values must be calculated for each simulation in turbine mode in order to plot the efficiency-flowrate curve and thus obtain the BEP for the turbine operation mode. Efficiency reveals how much energy in the inlet of the pump in turbine mode, is converted in mechanical energy by means of rotational speed of the shaft. This value is calculated by dividing the mechanical power generated in all the surfaces of the impeller (Equation 48) and the energy difference between discharge (PAT'inlet) and suction (PAT's outlet) parts of the machine as shown in equation 52

$$\eta = \frac{P_m}{P_{out} - P_{in}} \tag{52}$$

P_m=Mechanical power in impeller [W]

P_{out}=Energy at outlet [W]

P_{in}= Energy at inlet [W]

Efficiency values for the pump operating as turbine at different flow rate values are

summarized in table 15

Table 15: Efficiency values for turbine operation

Q $\left[\frac{m^3}{s}\right]$	Eff.$[\%]$
0.010	34.4
0.011	42.1
0.012	45
0.014	42.4
0.015	40.8
0.020	31.9

There can be seen that the efficiency for turbine mode grows up to the value of 45% at a mass flow rate of 12 $\frac{kg}{s}$ $\left(Q = 0.012\frac{m^3}{s}\right)$. In figure 47 it can be seen clearly, while the flow rate deviates from the BEP , the behavior of the efficiency decreases Efficiency is not as high as pump mode because pumps are designed for one direction of operation (from suction to discharge). In reverse operation efficiency might be less because of the shape of the impeller vanes

Figure 47: Turbine efficiency curve

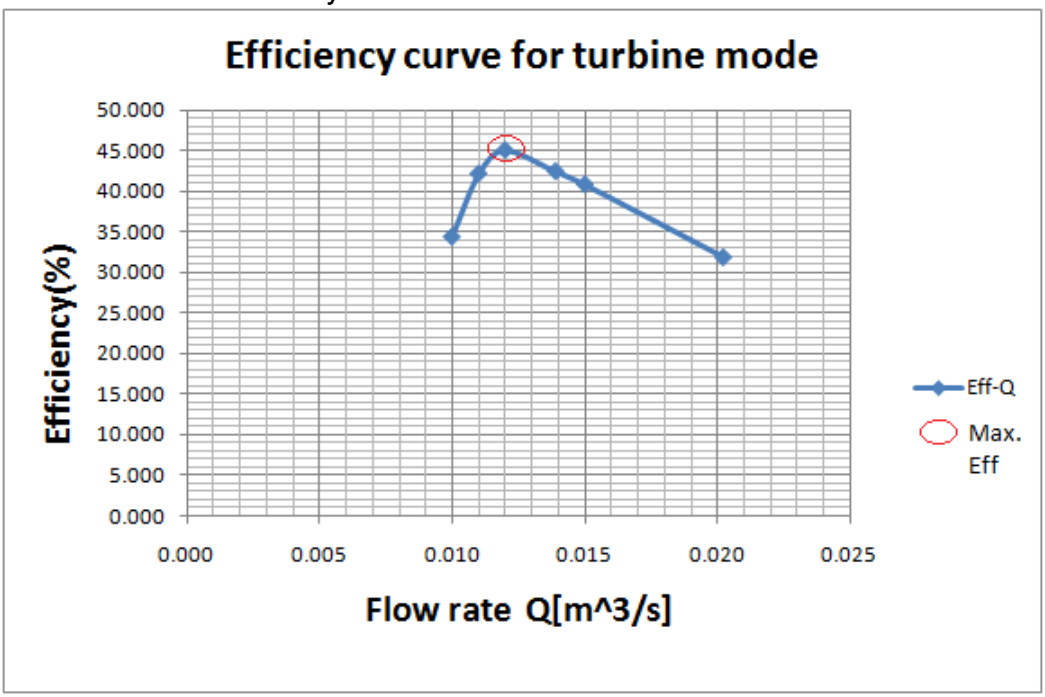

This point of maximum energy for the tested values of flow rate, is the BEP in which the pump is intended to operate. Now, after this value was achieved it is important to find the values for the mechanical power in each one of the simulations to see whether they fulfill the requirement of remaining below than electric power of the motor. Mechanical power is found applying equation 48. The value for the torque can be calculated inside the post–processing tool of the software as in equation 47, in simulation section (7).

Values for mechanical power found in each simulation are summarized in table 16

Table 16: Mechanical Power for turbine operation

Q $\left[\frac{m^3}{s}\right]$	Mechanical power CFD$[W]$
0.010	524.86
0.011	812.79
0.012	**1086.38**
0.014	1562.77
0.015	1818.93
0.020	3276.75

Mechanical power is $1086.38[W] = 1.45[HP]$ confirming that this is doubtless the BEP for this kind of pump at provided head, flow rate and rotational speed, because the value is kept below the requirement of electrical power of the motor.

According to theoretical methods, there exist no appropriate relationship between the simulation values and the experimental methods described in previous chapter. This reveals there is not an exact procedure for prediction of BEP for a pump operating in turbine mode and experimentation must be considered.

The curve for the pump operating in turbine is plotted and found BEP is shown in figure 48.

Figure 48: Turbine operation curve

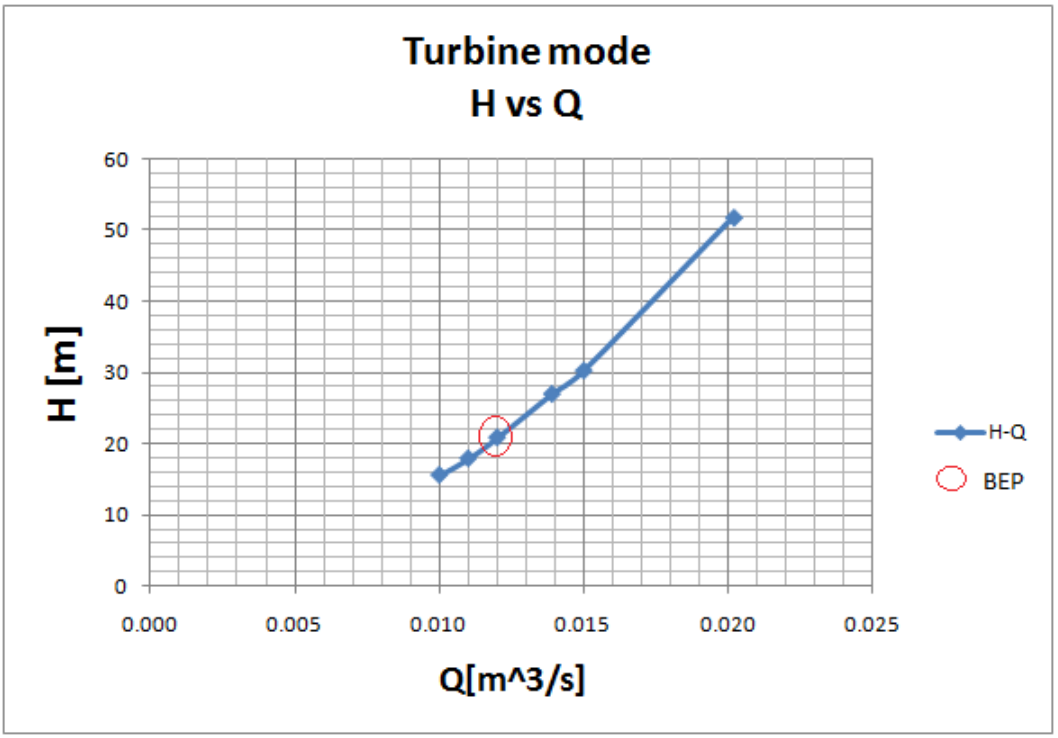

Regarding to graphical results, streamlines as well as vector and pressure fields will be plotted for flow rate values at BEP and over and below BEP. The way to plot these results is with the ratio between a value above and below and the flow rate at BEP in this manner:

$$Q_r = \frac{Q}{Q_{bep}}$$

These values will be:

$$Q = 0.010\,(Q_r = 0.83)\,, Q_{bep} = 0.012\,(Q_r = 1)\,, Q = 0.015\,(Q_r = 1.25)$$

.

Streamlines of the pump in turbine operation can be seen at different values for flow rate as stated.

Figure 49: Streamlines plot for turbine mode

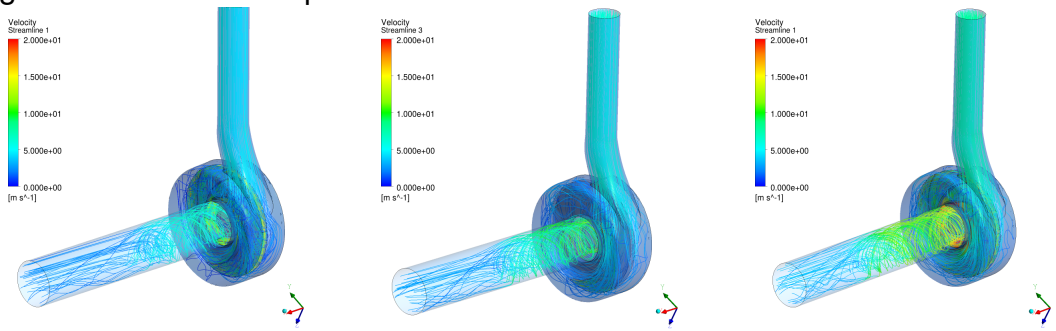

(a) Streamlines at $Q_r = 0.83$ (b) Streamlines at $Q_r = 1$ (c) Streamlines at $Q_r = 1.25$

In figure 49 there can be seen that swirl phenomena is present at the outlet of the pump becoming greater at higher values for flow rate. At $Q_r = 1(BEP)$ behavior of the flow is more uniform in the volute and despite there exists swirl, it stabilizes faster than other two conditions. Acceleration at leading edge combined with the movement of the impeller, results in a swirl at the impeller eye. For BEP, vectors in the outlet zone of the pump reveal this swirl behavior (figure 50)

Figure 50: Swirl vectors at impeller's eye (BEP)

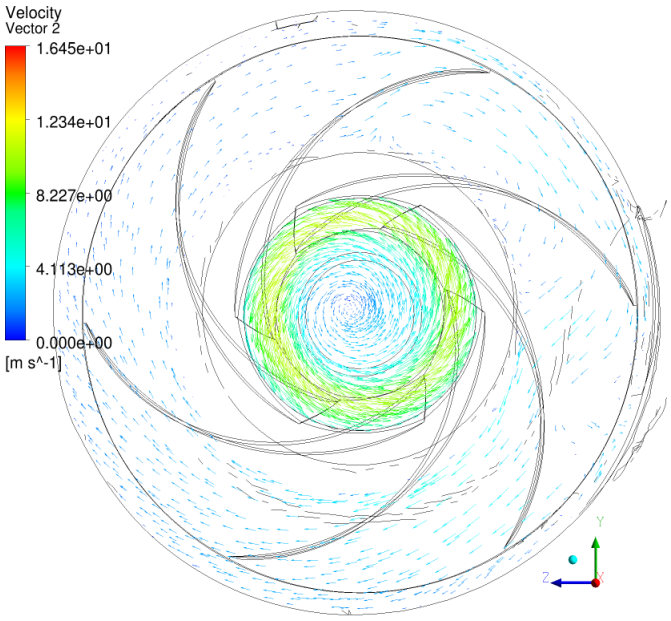

Pressure field for these conditions reveal the same behavior at different values of flow rate.

Figure 51: Pressure distribution for turbine mode

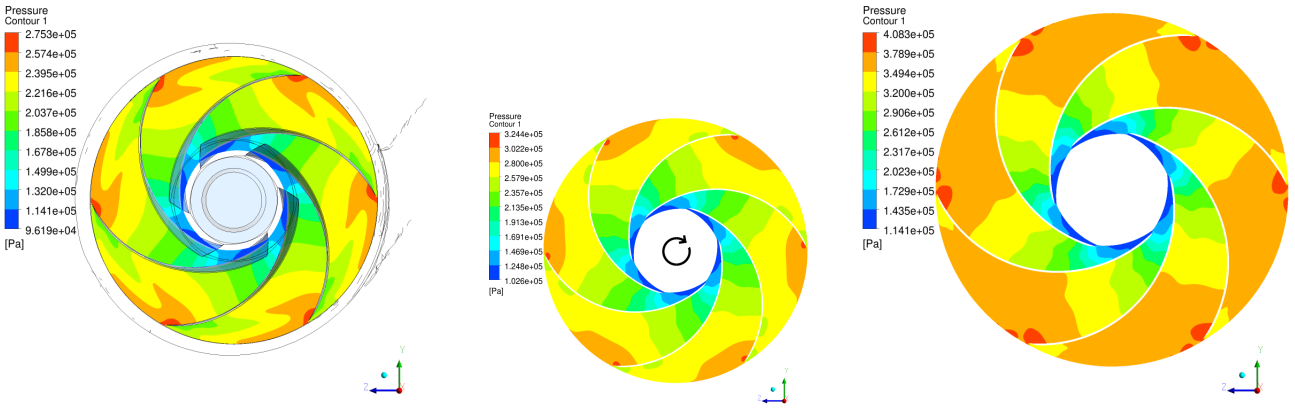

(a) Pressure at $Q_r = 0.83$ (b) Pressure at $Q_r = 1$ (c) Pressure at $Q_r = 1.25$

High pressure at the trailing edge of the vanes reveals that the fluid velocity in these zones is low because the flow hits the opposite side of the vane and “bounces” as an effect of the impulse it gives to the vane. Rotation of the impeller is reversed in pump mode, so it rotates clockwise as seen in figure 52

Figure 52: Turbine mode at BEP pressure

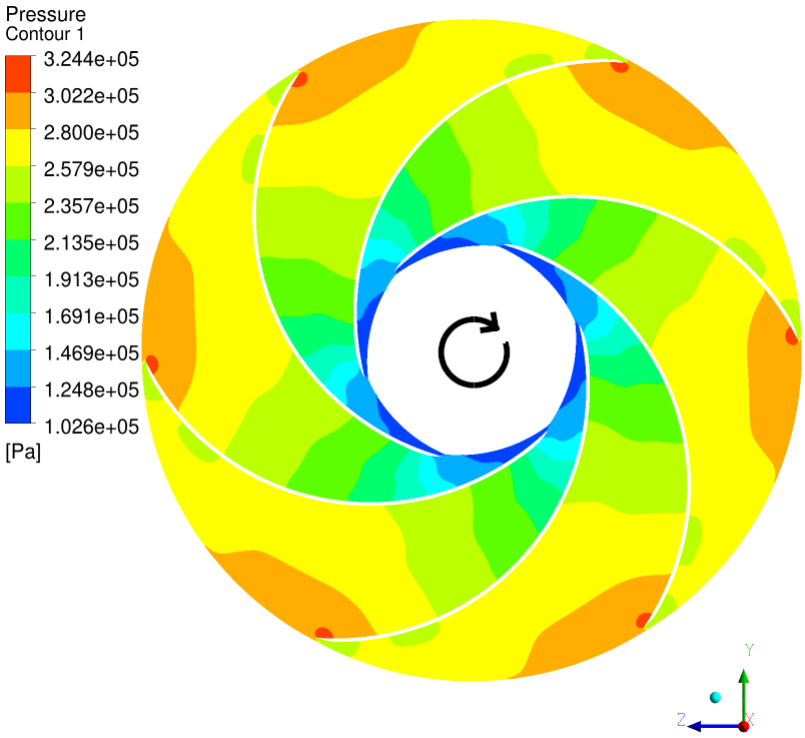

It can be seen that at BEP $Q_r = 1$ the pressure at trailing edge is less than other conditions (figure 52)revealing the fluid acquires more velocity following the curvature of the vane.

In Figure 53, velocity vectors for each conditions can be seen.

Figure 53: Velocity vector field for turbine mode

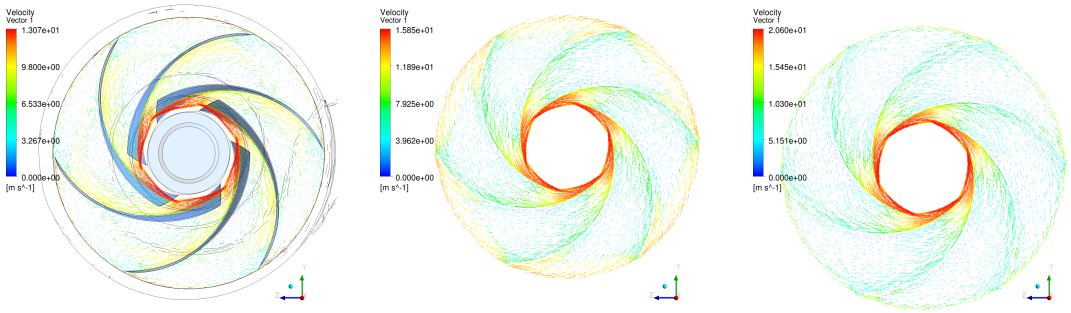

(a) Velocity vector field at $Q_r = 0.83$

(b) Velocity vector field at $Q_r = 1$

(c) Velocity vector field at $Q_r = 1.25$

Velocity field indicates that according the shape of the duct, velocity increases as it crosses the duct because the reduction of transversal area. The velocity increases following the curvature of the vane that is opposed to the vane hit by the flow. At $Q_r = 0.83$ the zone where flow hits the impeller shows little recirculation because of the energy cease after the impact.This is seen in figure 54

Figure 54: Little recirculation at trailing edge $Q_r = 0.83$

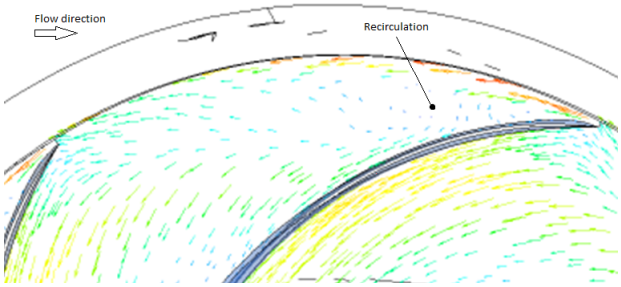

At $Q_r = 0.83$, large separation can be also seen in the middle of duct between vanes. This zone presents low velocity and recirculation of flow, leading to a high energy loss that can be revealed by means of the low efficiency value at this point of operation. Because separation phenomena is hard to visualize, the creation of sur-

face streamlines in the middle plane of the impeller, permitted good representation of recirculation flow due to separation as seen in figure 55

According to Sedlář, global separations are characterized by the presence of a saddle point in combination with a nodal point of attachment, accompanied often with, horn-type dividing surfaces (SEDLÁŘ et al., 2009).

Figure 55: Large separation at $Q_r = 0.83$

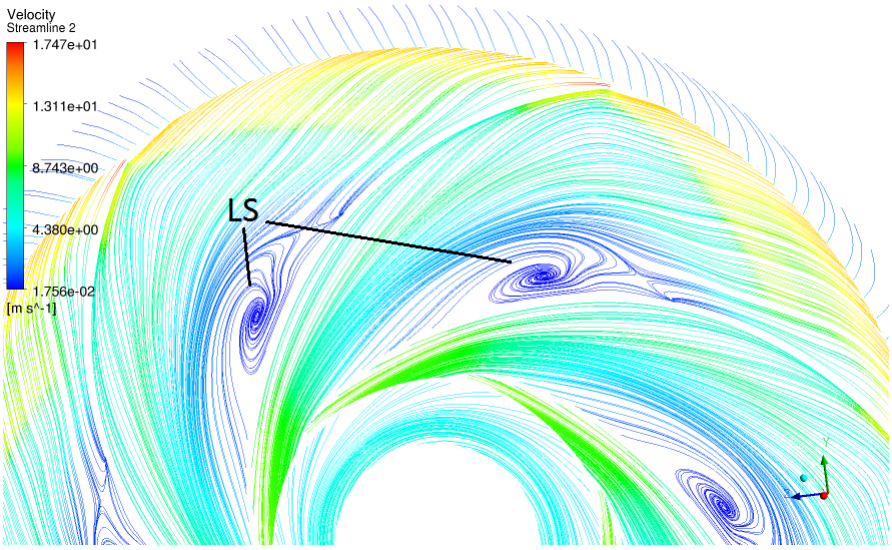

No separation was observed for the other cases (figure 56).

Figure 56: No separation at BEP and higher condition

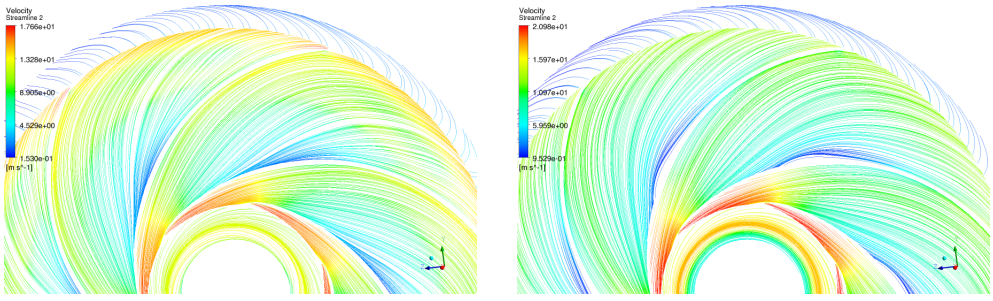

(a) No separation at $Q_r = 1$

(b) No separation at $Q_r = 1.25$

8.3 **Conclusions of the chapter**

The following are the conclusions for chapter 7

1. After simulating several conditions for flow rate, the best efficiency point of the pump operating in turbine mode is found at $Q = 0.012 \left[\frac{m^3}{s}\right]$, $H = 20.29\,[m]$ and efficiency value of 45%

2. Experimental prediction of BEP did not match with simulated data, being fundamental to compare simulation values with experimentation.

3. Boundary layer separation phenomena was observed inside the impeller at $Q = 0.010 \left[\frac{m^3}{s}\right]$ $(Q_r = 0.83)$. This behavior is supported by the low efficiency value for this flow condition (34.4%) resulting in low performance for the pump in reverse mode at this value.

4. At Best efficiency point the pump is able to convert available energy from the flow at inlet into mechanical energy in the shaft, preserving the value below the maximum required of $1185[W]$

9 CONCLUSIONS

This stage of the process reveals how the understanding of the project influenced the author to begin a quest through a field that has not been studied in depth, reversible principle of centrifugal pumps for energy generation.

Since the first steps of the project few problems were found and afforded with attitude. Reverse engineering process, presented a hard task to be completed: Acquisition of CAD models from the physical model of the centrifugal pump. In spite of little experience with digitizing techniques and demanding work in reconstruction of the models, the process was completed in a successful manner, obtaining CAD models of high quality.

After working with two different digitizing techniques, the author recommends the use of laser scanning method in order to obtain a digital model with higher resolution and in less time. Results with both techniques showed no considerable deviation in dimension regarding to real models. Manipulation of several CAD software permitted a simplification of the models without sacrificing the good quality from the reverse engineering process.

In the meshing process the creation of meshes with hexahedrical elements permitted the capture of separation phenomena between impeller's vanes. In order to minimize processing time, the construction of a mesh independence analysis provided information about how many elements can be used to produce similar results. This analysis showed that for a mesh of medium quality (around 1.5 million of elements)

was the most suitable for the simulations.

Regarding to simulation process it is necessary to state, that despite there is no need to focus on the mathematical model, correct definition of the variables involved in the process and the phenomena is required to save time and perform the CFD analysis with more accuracy.

Control points were used for monitoring of the simulation and the achievement of convergence and correct values along the iterations of the model. The SST model becomes an accurate model to provide valid data when, as this case, there exist no experimental values for setting a comparison.

The application of analytical procedures for finding the best efficiency for the pump operating in turbine mode were not exact at all, evidencing that it is from great importance to afford experimental measurements for comparison with the present case.

After simulating several conditions for flow rate, the best efficiency point of the pump operating in turbine mode was found at $Q = 0.012 \left[\frac{m^3}{s}\right]$ and $H = 20.29\,[m]$ corresponding to a efficiency value of 45% Mechanical power in the pump shaft was found to be $1086.38[W] = 1.45[HP]$ for obtained values at BEP. This value for power as well as encountered efficiency reinforce that BEP was achieved. Non tangential inflow through the impeller at low values for flow rates permitted the visualization of large separation in the pump when operated in turbine mode. This behavior reveals decrement of efficiency due to energy loss at these zones.

CFD is a complex process and this is the first serious approach to this method. Considerations of time , available computational resources and management of great

amount of data, limited the project becoming important to make recommendations for further work.

10 RECOMMENDATIONS

Some recommendations for the project are given to any person interested in the completion of the project:

1. It is from great importance to make experimental measurements of the real situation for the pump in order to acquire data and be able to compare these with simulations.

2. When possible, it should be a good practice to evaluate more conditions for different values of flow rate.

3. Better results can be achieved after having all the documentation and planning of the installation of the pump.

4. New simulations can be carried out taking into account losses from all components of the pump as well as pipes and control devices in the installation.

5. CFD results are approximate and might not be valid until a comparison with experimentation is made.

BIBLIOGRAPHY

ANSYS. Documentation for Ansys CFD package. http://www.ansys.com, 2009.

AUDISIO, Orlando. Bombas utilizadas como turbinas. http://fain.uncoma.edu.ar/centraleshidraulicas/archivos/PCH-BOMBAS%20COMO%20TURBINAS.PDF, 2009.

BAKKER, André. Boundary conditions notes from lecture in applied CFD, 2002. Fluent Inc.

CFDOnline. CFD Online interactive research community, 2009.

DERAKHSHAN, Shahram and NOURBAKHSH, Ahmad. Theoretical, numerical and experimental investigation of centrifugal pumps in reverse operation. in Experimental Thermal and Fluid Science vol. 32, 2008.

GOULDS. Goulds Centrifugal Pump Fundamentals. http://www.gouldspumps.com/download_files/pump_fundamentals/pf_fullindex.stm, 2009.

KARASSIK, Igor; MESSINA, Joseph; COOPER, Paul and HEALD, Charles. Pump Handbook 4 ed. Mc Graw Hill, New York, 2008.

KECK, Helmut and SICK, Mirjam. Thirty years of numerical flow simulation in hydraulic turbomachines. in Acta Mechanica vol. 201, 2008.

LANGE, Carlos. Discretization methods for ODE's and PDE's. Applied CFD course. http://www.mece.ualberta.ca/Courses/mec539/FDM_FEM_FVM.pdf, .

MENTER, Florian; KUNTZ, Martin and LANGTRY, Robin. Ten Years of Industrial Experience with the SST Turbulence Model. in Turbulence, Heat and Mass Transfer vol. 4, 2003.

MOTT, Robert. Applied Fluid Mechanics 6 ed. Prentice Hall, USA, 2006. ISBN 978-0131146807.

MUNSON, Bruce; YOUNG, Donald and OKIISHI, Theodore. Fundamentos de Mecanica de Fluidos 1 ed. Wiley, Mexico D.F, 2002. ISBN 968-18-5042-4.

ORREGO, Santiago. Estudio del comportamiento y caracterización de una turbina Francis usando CFD. Master thesis EAFIT University Medellín-Colombia, 2009.

ORTIZ, Ramiro and ABELLA, Jorge. Máquinas Hidráulicas Reversibles Aplicadas a Micro Centrales Hidroeléctricas. in IEEE Latin America Transactions vol. 6, 2008.

POLO, Manuel. Turbomaquinas Hidraulicas 2 ed. Limusa, Mexico DF, 1980.

PUMPWORLD. Pump World: Pump concepts. `http://www.pumpworld.com/contents.htm`, 2009.

RAJA, Vinesh and FERNANDES, Kiran. Reverse engineering: an industrial perspective. Springer, London, 2008 242 p.

RAWAL, Sonia and KSHIRSAGAR, J.T. Numerical simulation on a pump in turbine mode, 2007.

SAHDEV, Mukesh. Centrifugal Pumps: Basics Concepts of Operation, Maintenance, and Troubleshooting, Part I. `http://www.maintenanceworld.com/Articles/engresource/centrifugalpumps.pdf`, 2009.

SEDLÁŘ, Milan; ŠOUKAL, Jiří and KOMÁREK, Martin. CFD Analysis of middle stage of multistage pump operating in turbine regime. in Engineering MECHANICS vol. 16, 2009.

SMITH, Nigel. Motors as generators for micro hydro power 2 ed. Practical action publishing, London, 2008. ISBN 978 185339 645 8.

STREET, Robert; WATTERS, Gary and VENNARD, John. Elementary Fluid Mechanics 7 ed. John Wiley & Sons, New York, 1996. ISBN 0-471-01310-2.

VEERSTEG, H.K and MALALASEKERA, W. Introduction to computational fluid dynamics: The finite volume method 1 ed. Longman, London, 1995.

WILLIAMS, Arthur. Pump as turbines: A user's guide 2 ed. Practical action publishing, London, 2003. ISBN 978 185339 567 3.